nature cell biology

LETTERS

https://doi.org/10.1038/s41556-020-0559-z

Check for updates

UFMylation maintains tumour suppressor p53 stability by antagonizing its ubiquitination

Jiang Liu[1,3], Di Guan[1,3], Maogong Dong[1], Jingjing Yang[1], Haibin Wei[2], Qian Liang[1], Lizhi Song[1], Lu Xu[1], Junjie Bai[1], Cui Liu[1], Jian Mao[1], Qian Zhang[1], Junzhi Zhou[1], Xiaoying Wu[1], Miao Wang[1] and Yu-Sheng Cong[1]✉

p53 is the most intensively studied tumour suppressor[1]. The regulation of p53 homeostasis is essential for its tumour-suppressive function[2,3]. Although p53 is regulated by an array of post-translational modifications, both during normal homeostasis and in stress-induced responses[2–4], how p53 maintains its homeostasis remains unclear. UFMylation is a recently identified ubiquitin-like modification with essential biological functions[5–7]. Deficiency in this modification leads to embryonic lethality in mice and disease in humans[8–12]. Here, we report that p53 can be covalently modified by UFM1 and that this modification stabilizes p53 by antagonizing its ubiquitination and proteasome degradation. Mechanistically, UFL1, the UFM1 ligase[6], competes with MDM2 to bind to p53 for its stabilization. Depletion of UFL1 or DDRGK1, the critical regulator of UFMylation[6,13], decreases p53 stability and in turn promotes cell growth and tumour formation in vivo. Clinically, UFL1 and DDRGK1 expression are downregulated and positively correlated with levels of p53 in a high percentage of renal cell carcinomas. Our results identify UFMylation as a crucial post-translational modification for maintenance of p53 stability and tumour-suppressive function, and point to UFMylation as a promising therapeutic target in cancer.

The tumour suppressor p53 is a central governor of various critical cellular processes, and its stability is modulated by a large number of post-translational modifications[4,14], such as ubiquitination and ubiquitin-like modifications[15–19]. However, the detailed molecular mechanisms controlling p53 stability both during normal homeostasis and stress-induced conditions remain incompletely understood[2–4]. The ubiquitin-fold modifier 1 (UFM1) conjugation system is a recently identified ubiquitin-like modification. As with ubiquitination, UFMylation is catalysed by the E1- and E2-like enzymes ubiquitin-like modifier activating enzyme 5 (UBA5) and ubiquitin-fold modifier-conjugating enzyme 1 (UFC1), and by the E3-like ligase UFM1-specific ligase 1 (UFL1)[5–7]. DDRGK domain-containing protein 1 (DDRGK1; also known as UFM1-binding protein 1 (UFBP1)) is a critical regulatory factor for UFMylation[13]. The significance of UFMylation is highlighted by its essential roles in endoplasmic reticulum homeostatic maintenance and embryonic development[9–11,20–22]. Yet, the substrates of UFMylation and its underlying biological functions remain poorly understood. Only a few substrates have so far been described[6,13,23–26]. Here, we screened for substrates of UFMylation by exploring the proteins that bind with UFL1 and DDRGK1 simultaneously (Extended Data Fig. 1a,b). Notably, the tumour suppressor p53 was found to be one of these candidate proteins because it presented in both UFL1 and DDRGK1 immunoprecipitates analysed by mass spectrometry (Supplementary Tables 1 and 2). Conversely, both UFL1 and DDRGK1 were found to be associated with p53 in our mass spectrometry analysis (Supplementary Table 3). Immunoprecipitation analysis further confirmed that UFL1, DDRGK1 and p53 were capable of binding to each other (Extended Data Fig. 1c–e). Importantly, endogenous UFL1, DDRGK1 and p53 indeed interacted with each other in cells (Fig. 1a and Extended Data Fig. 1f,g). Furthermore, our in vitro binding assays (Fig. 1b,c) showed that p53 directly interacted with UFL1 and DDRGK1, suggesting that p53 could be a bona fide substrate of UFMylation.

To determine whether p53 can be UFMylated, we coexpressed p53 in HEK293T cells with the UFMylation components UBA5, UFC1, UFL1, UFM1 and DDRGK1. The in vivo UFMylation assays showed that wild-type UFM1 ($UFM1^{WT}$) and an active form of UFM1 with an exposed carboxy (C)-terminal glycine 83 residue ($UFM1^{\Delta C2}$), but not an inactive form of UFM1 lacking the C-terminal glycine 83 residue ($UFM1^{\Delta C3}$)[5], could conjugate to p53 (Fig. 1d). Furthermore, we confirmed that UFMylation modification of endogenous p53 can be detected in both human cancer cells and primary mouse embryonic fibroblast (MEF) cells (Fig. 1e,f). In addition, our in vitro UFMylation assays further demonstrated that p53 is indeed a substrate of UFMylation (Fig. 1g). Interestingly, we noted that UFMylated p53 could be detected in cells without overexpression of UBA5, but required overexpression of UFC1, UFL1 and DDRGK1 (Extended Data Fig. 2a). Consistently, knockdown of UFC1, UFL1 and DDRGK1 decreased p53 UFMylation, whereas knockdown of UBA5 had no significant effect (Extended Data Fig. 2b–e). A similar observation was reported for ASC1 UFMylation[13]. However, in vitro UFMylation assays showed that the UFMylation components UBA5, UFC1, UFL1, UFM1 and DDRGK1 were all required for p53 modification (Fig. 1g). This suggests that UBA5 is required for p53 UFMylation but is not a limiting factor in cells. Altogether, these data demonstrate that p53 can be UFMylated both in vivo and in vitro.

To identify the UFMylation sites in p53, we generated lysine-to-arginine (Lys-to-Arg) mutations in various combinations (Extended Data Fig. 3a). Of these, only the mutants K351/357 (where all Lys residues except Lys351 and 357 were replaced by Arg) and K370–386 (where all Lys residues except 370, 372, 373, 381, 382 and 386 were replaced by Arg) allowed UFMylation of p53, indicating that the p53 UFMylation sites reside in these Lys residues (Extended Data Fig. 3b). As there are eight Lys residues

[1]Key Laboratory of Aging and Cancer Biology of Zhejiang Province, Institute of Aging Research, School of Medicine, Hangzhou Normal University, Hangzhou, China. [2]Institute of Cancer and Basic Medicine, Cancer Hospital of the University of Chinese Academy of Sciences, Zhejiang Cancer Hospital, Hangzhou, China. [3]These authors contributed equally: Jiang Liu, Di Guan. ✉e-mail: yscong@hznu.edu.cn

in the K351/357 and K370–386 mutants, we generated each single Lys-to-Arg mutation and found that the replacement of Lys351, 357, 370 or 373 individually by Arg reduced p53 UFMylation (Extended Data Fig. 3c). To confirm this finding, we substituted all Lys residues by Arg in p53 except one each of these four residues (Lys351, 357, 370 or 373) and found that these four residues can be individually UFMylated, albeit less efficiently than wild-type p53 (Extended Data Fig. 3d). $p53^{20KR}$—the Lys-less mutant—was used as a negative control (Extended Data Fig. 3b–d). In addition, the replacement of all of these four lysine residues by Arg (referred to as 4KR) significantly reduced p53 UFMylation in vivo and in vitro (Fig. 1h,i). Based on the molecular weight of UFMylated p53, we assumed that p53 was modified by mono-UFM1. Indeed, we observed that modification of p53 by $UFM1^{WT}$ was similar to that by $UFM1^{K0}$ (the Lys-less mutant) (Fig. 1j), which can only form mono-UFM1 modification[13]. Based on these analyses, we concluded that p53 can be modified by mono-UFM1 at the four Lys residues (Lys351, 357, 370 or 373) in its C-terminal region. However, this does not exclude other Lys residues from being potentially UFMylated under particular physiological conditions in response to intrinsic and extrinsic stresses.

To investigate the regulation of p53 by UFMylation, we depleted UFL1 or DDRGK1 in HCT116, U2OS and HeLa cells by specific small interfering RNAs (siRNAs), and found that knockdown of UFL1 or DDRGK1 significantly decreased p53 protein levels without affecting p53 messenger RNA levels, while both protein and messenger RNA levels of p21 (a canonical p53 target) were decreased (Fig. 2a and Extended Data Fig. 4a,b). We then examined the effect of UFMylation on p53 stability in cells treated with cycloheximide and found that p53 stability was reduced after depletion of UFL1 or DDRGK1 (Fig. 2b and Extended Data Fig. 4c,d). Treatment of the cells with the proteasome inhibitor MG132 prevented p53 degradation induced by knockdown of UFL1 or DDRGK1 (Extended Data Fig. 4e,f), suggesting that UFMylation maintains p53 protein stability by competing with ubiquitination. Indeed, the ubiquitination of endogenous p53 was significantly increased by knockdown of UFL1 or DDRGK1 in cells (Fig. 2c). Conversely, we found that increased levels of UFMylation by overexpressing its components result in decreased ubiquitination of $p53^{WT}$ (Fig. 2d), indicating that p53 UFMylation antagonized its ubiquitination. As the four UFMylation lysine residues of p53 are also reported as ubiquitination sites[27–29], we then examined the ubiquitination of $p53^{4KR}$ and found that ubiquitination of the $p53^{4KR}$ mutant was decreased compared with that of $p53^{WT}$, and this decreased ubiquitination was not affected by overexpressing the UFMylation components (Fig. 2d). Therefore, p53 UFMylation might interdict its ubiquitination and proteasome degradation through these four lysine residues.

To explore the antagonistic mechanism between p53 UFMylation and its ubiquitination, we generated different truncations of p53 to examine the interaction between p53 and UFL1. We found that p53 lacking an amino (N)-terminal region failed to associate with UFL1, indicating that the N-terminal region of p53 is responsible for UFL1 binding (Fig. 2e), and this region is also known for mouse double minute 2 homologue (MDM2) binding[30]. As MDM2 is the principal E3 ligase for p53 degradation[4], we speculated that UFL1 might compete with MDM2 for binding to p53 and stabilize p53 by UFMylation. Consistent with this hypothesis, depletion of UFL1 promoted the interaction of p53 with MDM2 (Fig. 2f). Additionally, in vivo and in vitro assays showed that the interaction of UFL1 with p53 gradually reduced as MDM2 increased (Fig. 2g,h). These results suggest that UFL1 competes with MDM2 for binding to p53, and subsequently leads to p53 UFMylation, thereby stabilizing p53 by counteracting its ubiquitination.

The DNA damage responses are critical mediators of p53-dependent tumour suppression. To explore the regulation of p53 UFMylation in response to DNA damage, we examined the UFMylation levels of p53 under DNA damage induced by doxorubicin or etoposide. The results showed that the UFMylation level of endogenous p53 was elevated upon DNA damage, whereas depletion of UFL1 or DDRGK1 significantly decreased p53 UFMylation and prevented p53 accumulation under DNA damage conditions (Fig. 3a). Consistently, p53 and p21 were upregulated upon DNA damage in a time-dependent manner, while knockdown of UFL1 or DDRGK1 prevented accumulation of p53 and p21 in both HCT116 cells and HeLa cells (Fig. 3b,c and Extended Data Fig. 5a–d). These results indicate that UFMylation is required for DNA damage-induced p53 accumulation. We thus investigated the effects of p53 UFMylation on cell growth upon DNA damage. We generated stable cell lines depleted of UFL1 or DDRGK1 expression by short hairpin RNA (shRNA) lentivirus infection (Extended Data Fig. 5e) and observed that HCT116 $p53^{+/+}$ cells stably depleted of UFL1 or DDRGK1 were proficient in colony formation (Fig. 3d), whereas colony formation was not affected in HCT116 $p53^{-/-}$ cells with UFL1 or DDRGK1 depletion (Fig. 3e), indicating that cell growth inhibition by p53 accumulation is dependent on its UFMylation. Furthermore, we generated stable cell lines expressing $p53^{WT}$ or $p53^{4KR}$ in HCT116 $p53^{-/-}$ cells (Extended Data Fig. 5f) and found that depletion of UFL1 resulted in increased cell growth in $p53^{WT}$-expressing cells upon DNA damage (Fig. 3f,g), but not in $p53^{4KR}$-expressing cells (Fig. 3h,i). Collectively, these findings demonstrated that UFMylation is responsible for p53 accumulation in response to DNA damage.

To further investigate the role of p53 UFMylation in its tumour-suppressive function in vivo, we performed mouse xenograft assays by injecting BALB/c nude mice with HCT116 cells stably depleted of UFL1 or DDRGK1 (Extended Data Fig. 5e,f). We found that depletion of UFL1 or DDRGK1 led to increased tumour size and weight in mice carrying HCT116 $p53^{+/+}$ cells (Fig. 4a–d) or HCT116 $p53^{-/-}$ cells expressing $p53^{WT}$ (Fig. 4e,f), but depletion of UFL1 or DDRGK1 had little effect on tumour growth in mice carrying HCT116 $p53^{-/-}$ cells (Fig. 4g–j) or HCT116 $p53^{-/-}$ cells expressing $p53^{4KR}$ (Fig. 4k,l). These results support a crucial role of p53 UFMylation in its tumour-suppressive function in vivo, and lead us

Fig. 1 | Identification of p53 as a target for UFMylation. a, Western blot analysis of the mutual interactions between UFL1, DDRGK1 and p53 in HEK293T cells by co-immunoprecipitation with p53 antibody. Mouse IgG was used as a control. **b**,**c**, In vitro binding assays between p53 and UFL1 or DDRGK1. **b**, Purified p53 was incubated with GST-tagged UFL1 or DDRGK1, followed by GST pulldown assay and western blot with anti-p53 antibody. **c**, Purified UFL1 or DDRGK1 was incubated with GST-p53 followed by GST pulldown assay and western blot with anti-HA or anti-DDRGK1 antibody. **d**, UFMylation of p53 was analysed by western blot with anti-UFM1 antibody in HEK293T cells expressing the UFMylation system components. **e**, UFMylation of endogenous p53 was analysed by immunoprecipitation with p53 antibody followed by western blot with anti-UFM1 antibody in HCT116 and U2OS cells in the presence of MG132 (20 μM; 8 h). **f**, UFMylation of endogenous p53 was analysed by immunoprecipitation with p53 antibody followed by western blot with the anti-UFM1 antibody in primary MEF cells, in the presence of MG132 (20 μM; 8 h). **g**, In vitro UFMylation of p53. Purified UFMylation components and p53 were incubated in UFMylation buffer. The reaction was terminated by adding SDS sample buffer, and the samples were subjected to western blot with anti-p53 antibody. **h**, UFMylation assay of the p53 wild type (WT) and its mutants in HEK293T cells expressing the indicated UFMylation system components. **i**, In vitro UFMylation assay of p53 and its mutants, as described in **g**. Us., UFMylation system components (consisting of E1, E2, E3, DDRGK1 and UFM1). **j**, The UFMylated form of p53 in HEK293T cells expressing the indicated UFMylation system components was analysed by western blot with anti-UFM1 antibody.

to propose that UFL1 and DDRGK1 also act as tumour suppressors. It has been reported that renal cell carcinomas (RCCs) have fewer p53 mutations[31,32]. We therefore collected 12 fresh frozen RCC tissues and confirmed that all samples contained wild-type *TP53* by exon sequencing. We then analysed the expression of UFL1, DDRGK1 and p53 in these samples, and found that the levels of UFL1 and DDRGK1 were significantly decreased in RCC samples compared with adjacent normal tissues, and positively correlated with levels of p53, except for one pair of tissues (Fig. 5a). In addition, RCC tissue microarray analysis from 40 paired samples confirmed

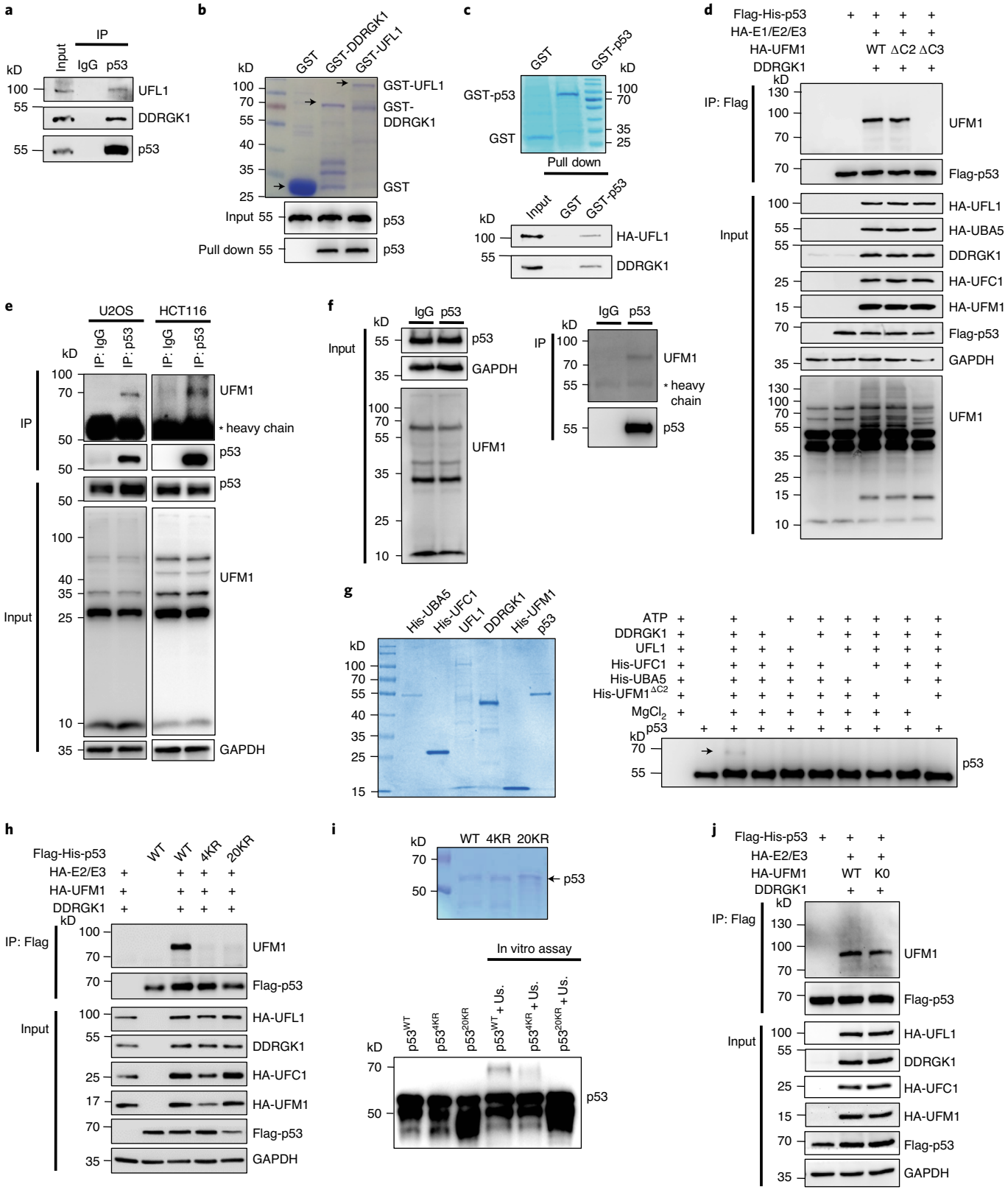

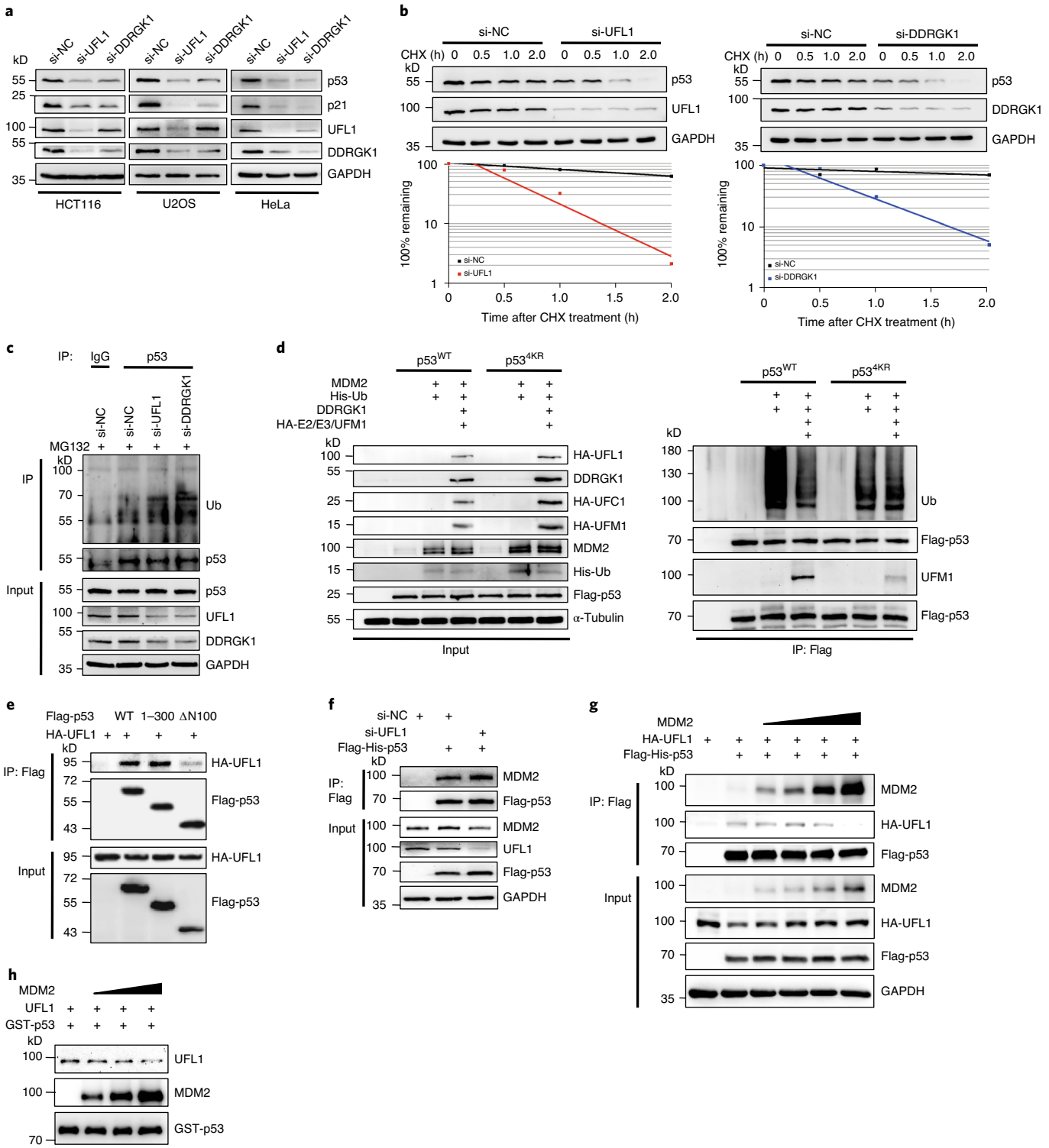

Fig. 2 | UFMylation stabilizes p53 by antagonizing its ubiquitination. a, Western blot analysis of p53 and p21 expression in HCT116, U2OS and HeLa cells with UFL1 or DDRGK1 depletion. **b**, p53 stability was examined by western blot in HCT116 cells with UFL1 or DDRGK1 depletion. The cells were treated with 100 μg ml^{-1} cycloheximide (CHX) for the indicated times. The graph represents quantification of the p53 protein levels. **c**, Ubiquitination of endogenous p53 was analysed by immunoprecipitation with p53 antibody and followed by western blot analysis in HCT116 cells with UFL1 or DDRGK1 depletion in the presence of MG132 (20 μM; 8 h). **d**, Western blot analysis of p53 UFMylation and ubiquitination in HEK293T cells with Flag-p53^{WT} or Flag-p53^{4KR} mutant expression. **e**, The binding region of p53 with UFL1 was identified by western blot in HEK293T cells with Flag-p53^{WT} and truncation expression. The Flag-p53 1–300 construct denotes the p53 cDNA with 93 amino acids deleted at the C terminus. The Flag-p53 ΔN100 construct denotes the p53 cDNA with 100 amino acids deleted at the N terminus. **f**, Western blot analysis of the interactions between MDM2 and p53 in HEK293T cells with UFL1 depletion. **g**,**h**, Western blot analysis of the interactions between UFL1 and p53 in HEK293T cells (**g**) and in vitro (**h**) with increased amounts of MDM2. NC, negative control; si-, small interfering RNA.

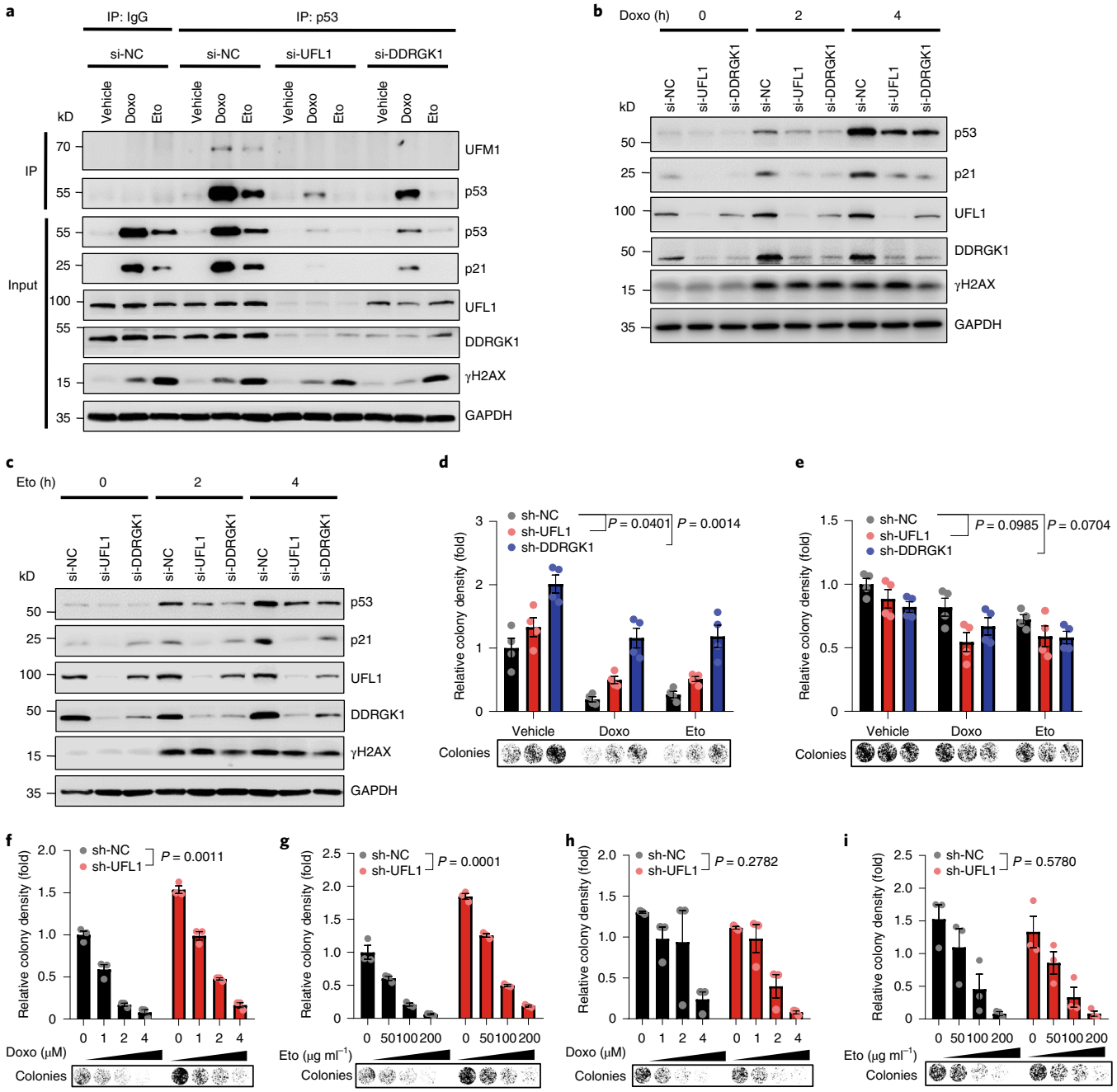

Fig. 3 | UFMylation is required for p53 accumulation in the DNA damage response. a, UFMylation of endogenous p53 was analysed by western blot in HCT116 $p53^{+/+}$ cells depleted of UFL1 or DDRGK1 upon DNA damage induced by doxorubicin (doxo; 1 μM; 24 h) or etoposide (eto; 25 μg ml^{-1}; 12 h). **b**,**c**, Western blot analysis of p53 and p21 expression in HCT116 $p53^{+/+}$ cells depleted of UFL1 or DDRGK1 in the presence of doxorubicin (1 μM) (**b**) or etoposide (25 μg ml^{-1}) (**c**) for the indicated times. **d**,**e**, Colony formation assay of HCT116 $p53^{+/+}$ (**d**) or HCT116 $p53^{-/-}$ (**e**) cells depleted of UFL1 or DDRGK1 under DNA damage conditions (doxorubicin: 2 μM; etoposide: 100 μg ml^{-1}) ($n = 4$ biologically independent experiments). **f**–**i**, Colony formation assays of $p53^{WT}$ stably expressed HCT116 $p53^{-/-}$ cells with UFL1 depletion in the presence of doxorubicin (**f**) and etoposide (**g**) or $p53^{4KR}$ stably expressed HCT116 $p53^{-/-}$ cells with UFL1 depletion in the presence of different doses of doxorubicin (**h**) and etoposide (**i**), as indicated ($n = 3$ biologically independent experiments). Top: analysis of colony density. Bottom: representative images of colonies. Error bars indicate means ± s.e.m. A two-way analysis of variance test was used for **d**–**i**.

that the majority showed lower expression of UFL1, DDRGK1 and p53 in cancer tissues compared with adjacent normal tissues (Fig. 5b and Extended Data Fig. 6a–d). The expression levels of UFL1 and DDRGK1 were positively correlated with those of p53 (Fig. 5c). Notably, we performed Kaplan–Meier analysis based on The Cancer Genome Atlas database, and found that the lower expression of UFL1 or DDRGK1 was closely associated with poorer overall survival in patients with kidney renal clear cell carcinoma (Fig. 5d,e). Taken together, these results suggest that UFL1 and DDRGK1 could function as tumour suppressors by modulating p53 stability.

Overall, our study shows that p53 is a bona fide substrate of UFMylation, and this modification maintains p53 stability by competing with MDM2-mediated ubiquitination, thereby contributing

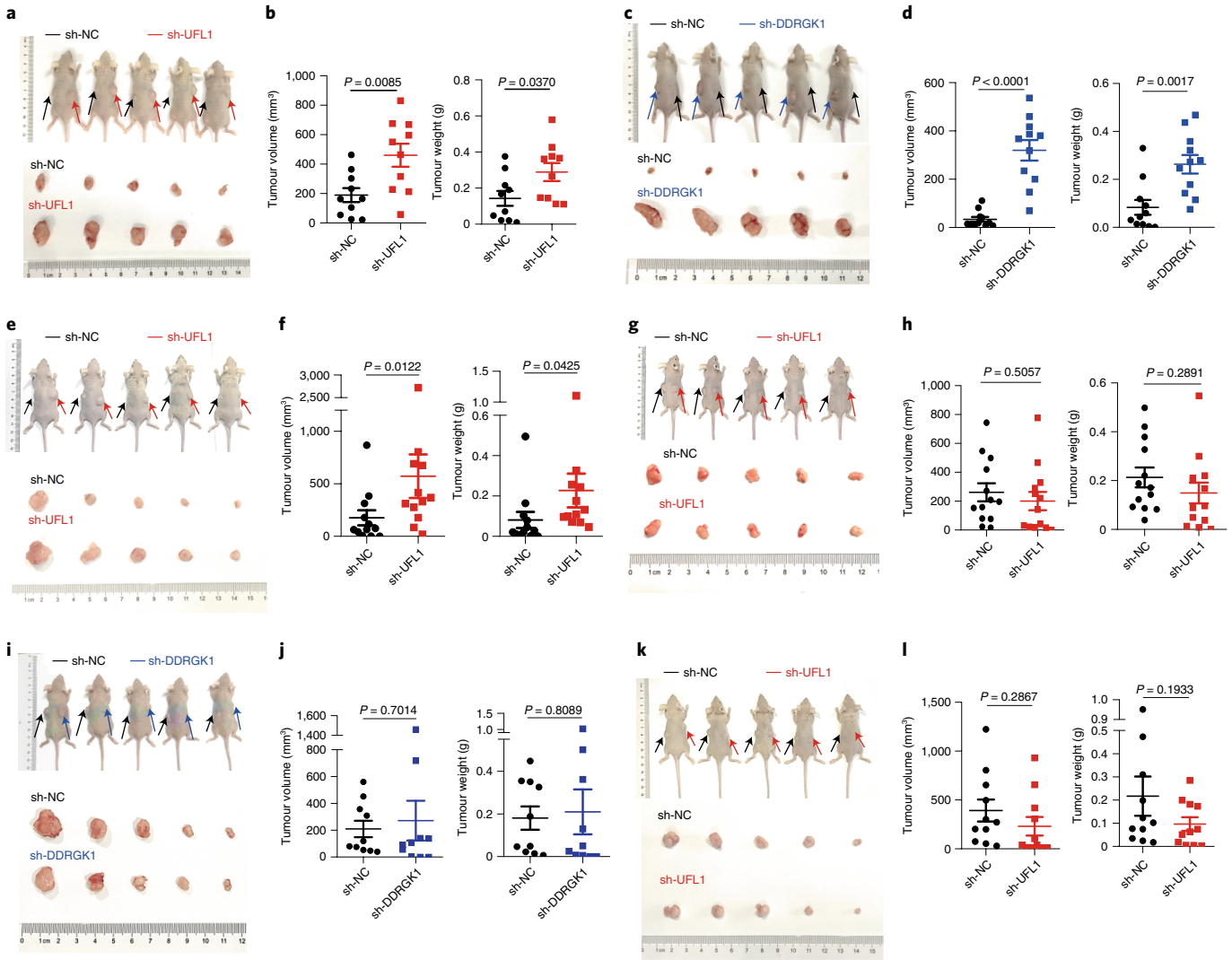

Fig. 4 | UFMylation maintains the tumour-suppressive function of p53. a–l, Xenograft analysis of tumour growth in mice carrying: HCT116 $p53^{+/+}$ cells with UFL1 (**a** and **b**; $n=10$) or DDRGK1 (**c** and **d**; $n=11$) depletion; HCT116 $p53^{-/-}$ cells stably expressing $p53^{WT}$ with UFL1 depletion (**e** and **f**; $n=12$); HCT116 $p53^{-/-}$ cells with UFL1 (**g** and **h**; $n=13$) or DDRGK1 (**i** and **j**; $n=10$) depletion; or HCT116 $p53^{-/-}$ cells stably expressing $p53^{4KR}$ with UFL1 depletion (**k** and **l**; $n=11$). Representative images of mice and tumours are shown (**a**, **c**, **e**, **g**, **i** and **k**), and the volume and weight of tumours were measured, respectively (**b**, **d**, **f**, **h**, **j** and **l**). Error bars indicate means ± s.e.m.

to p53 tumour-suppressive function (Fig. 5f). Our results point to UFMylation as an attractive potential target for cancer therapy.

p53 has the capacity to regulate the expression of several hundred genes involved in regulating cell growth, division, survival and cell death[33], and plays a central role in multiple cellular stress responses. Under normal homeostatic conditions, p53 is a short-lived protein[34]. However, under diverse cellular stresses, p53 is stabilized primarily through post-translational mechanisms to act as a tumour suppressor that promotes growth arrest, senescence or apoptosis, providing a critical barrier to uncontrolled proliferation of transformed cells[2]. Thus, the mechanisms leading to p53 activation also constitute a crucial component of tumour suppression that prevents oncogenic conversion of damaged cells. In the context of DNA damage, p53 is a decision-making transcriptional factor that determines the cellular outcome. Our results showed that UFMylation is responsible for p53 accumulation in response to DNA damage. In line with these findings, it has been reported recently that UFL1 is phosphorylated and recruited to double-strand breaks, where it mono-UFMylates histone H4 and enhanced Suv39h1 and Tip60 recruitment, which promotes the ataxia-telangiectasia mutated (ATM) kinase activation upon DNA damage[24]. Similarly, UFMylation of MRE11 was found to be required for MRE11–RAD50–NBS1 (MRN) complex formation and appropriate coordinated DNA damage repair[23]. Together, these findings underscore a crucial role of UFMylation modification in the process of DNA damage response and the maintenance of genomic integrity.

p53 can be post-translationally modified by multiple mechanisms including phosphorylation, acetylation, methylation, SUMOylation, NEDDylation and ubiquitination in response to a wide variety of intrinsic and extrinsic stresses[35]. However, there is relatively limited information about where and when in the cells these modifications take place, and how different modifications are coordinated. The finding that p53 is a substrate of UFMylation modification adds additional levels of complexity to the regulation of p53 responses. We found that p53 can be modified by mono-UFM1 at four Lys residues (Lys351, 357, 370 or 373) in its C-terminal region. These Lys residues are also subject to acetylation and ubiquitination[4,28,29,36]. How UFMylation interacts with other modifications with regard to p53 homeostasis or its specific activity under normal homeostasis or specific stress conditions therefore merits detailed future investigation.

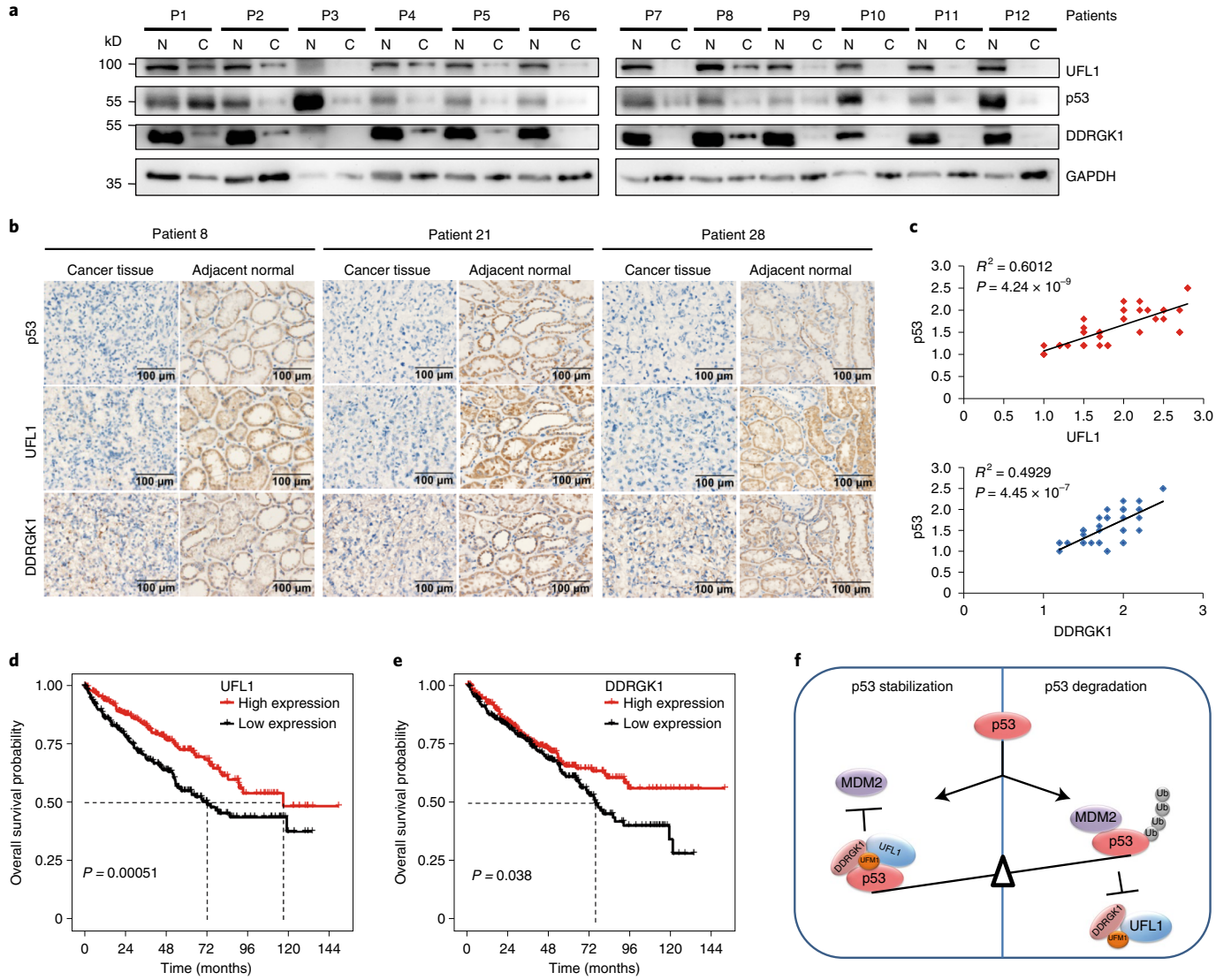

Fig. 5 | UFL1 and DDRGK1 expression are downregulated and positively correlated with levels of p53 in RCC. a, Western blot analysis of UFL1, DDRGK1 and p53 expression in 12 pairs of fresh frozen RCC tissues and the corresponding adjacent tissues. C, cancer tissue; N, normal tissue. **b**, Representative sections of immunohistochemical staining of UFL1, DDRGK1 and p53 in 40 pairs of RCC and adjacent normal tissues in tissue array. **c**, Correlation analysis of UFL1 ($P = 4.24 \times 10^{-9}$; $R^2 = 0.6012$) and DDRGK1 ($P = 4.45 \times 10^{-7}$; $R^2 = 0.4929$) versus p53 expression in 40 pairs of RCC and adjacent normal tissues in tissue array. **d**,**e**, Kaplan–Meier curves of overall survival in patients with kidney renal clear cell carcinoma who were stratified for low UFL1 (**d**) and DDRGK1 (**e**) versus high UFL1 (**d**) and DDRGK1 (**e**) expression ($n = 529$ independent patient samples; UFL1: $P = 0.00051$; DDRGK1: $P = 0.038$). Data were obtained from The Cancer Genome Atlas. **f**, Working model of UFMylation controlling p53 stability.

Online content

Any methods, additional references, Nature Research reporting summaries, source data, extended data, supplementary information, acknowledgements, peer review information; details of author contributions and competing interests; and statements of data and code availability are available at https://doi.org/10.1038/s41556-020-0559-z.

Received: 18 July 2019; Accepted: 14 July 2020;
Published online: 17 August 2020

References

1. Dolgin, E. The most popular genes in the human genome. *Nature* **551**, 427–431 (2017).
2. Kastenhuber, E. R. & Lowe, S. W. Putting p53 in context. *Cell* **170**, 1062–1078 (2017).
3. Vousden, K. H. & Prives, C. Blinded by the light: the growing complexity of p53. *Cell* **137**, 413–431 (2009).
4. Kruse, J. P. & Gu, W. Modes of p53 regulation. *Cell* **137**, 609–622 (2009).
5. Komatsu, M. et al. A novel protein-conjugating system for Ufm1, a ubiquitin-fold modifier. *EMBO J.* **23**, 1977–1986 (2004).
6. Tatsumi, K. et al. A novel type of E3 ligase for the Ufm1 conjugation system. *J. Biol. Chem.* **285**, 5417–5427 (2010).
7. Daniel, J. & Liebau, E. The ufm1 cascade. *Cells* **3**, 627–638 (2014).
8. Nahorski, M. S. et al. Biallelic *UFM1* and *UFC1* mutations expand the essential role of UFMylation in brain development. *Brain* **141**, 1934–1945 (2018).
9. Tatsumi, K. et al. The Ufm1-activating enzyme Uba5 is indispensable for erythroid differentiation in mice. *Nat. Commun.* **2**, 181 (2011).
10. Zhang, M. et al. RCAD/Ufl1, a Ufm1 E3 ligase, is essential for hematopoietic stem cell function and murine hematopoiesis. *Cell Death Differ.* **22**, 1922–1934 (2015).
11. Cai, Y. et al. UFBP1, a key component of the Ufm1 conjugation system, is essential for UFMylation-mediated regulation of erythroid development. *PLoS Genet.* **11**, e1005643 (2015).

12. Egunsola, A. T. et al. Loss of DDRGK1 modulates SOX9 ubiquitination in spondyloepimetaphyseal dysplasia. *J. Clin. Invest.* **127**, 1475–1484 (2017).
13. Yoo, H. M. et al. Modification of ASC1 by UFM1 is crucial for ERα transactivation and breast cancer development. *Mol. Cell* **56**, 261–274 (2014).
14. Gu, B. & Zhu, W. G. Surf the post-translational modification network of p53 regulation. *Int. J. Biol. Sci.* **8**, 672–684 (2012).
15. Honda, R., Tanaka, H. & Yasuda, H. Oncoprotein MDM2 is a ubiquitin ligase E3 for tumor suppressor p53. *FEBS Lett.* **420**, 25–27 (1997).
16. Scheffner, M., Huibregtse, J. M., Vierstra, R. D. & Howley, P. M. The HPV-16 E6 and E6-AP complex functions as a ubiquitin–protein ligase in the ubiquitination of p53. *Cell* **75**, 495–505 (1993).
17. Huang, Y. F., Wee, S., Gunaratne, J., Lane, D. P. & Bulavin, D. V. Isg15 controls p53 stability and functions. *Cell Cycle* **13**, 2200–2210 (2014).
18. Weger, S., Hammer, E. & Heilbronn, R. Topors acts as a SUMO-1 E3 ligase for p53 in vitro and in vivo. *FEBS Lett.* **579**, 5007–5012 (2005).
19. Maki, C. G., Huibregtse, J. M. & Howley, P. M. In vivo ubiquitination and proteasome-mediated degradation of p53. *Cancer Res.* **56**, 2649–2654 (1996).
20. Lemaire, K. et al. Ubiquitin fold modifier 1 (UFM1) and its target UFBP1 protect pancreatic beta cells from ER stress-induced apoptosis. *PLoS ONE* **6**, e18517 (2011).
21. Liu, J. et al. A critical role of DDRGK1 in endoplasmic reticulum homoeostasis via regulation of IRE1α stability. *Nat. Commun.* **8**, 14186 (2017).
22. Li, J. et al. Ufm1-specific ligase Ufl1 regulates endoplasmic reticulum homeostasis and protects against heart failure. *Circ. Heart Fail.* **11**, e004917 (2018).
23. Wang, Z. et al. MRE11 UFMylation promotes ATM activation. *Nucleic Acids Res.* **47**, 4124–4135 (2019).
24. Qin, B. et al. UFL1 promotes histone H4 UFMylation and ATM activation. *Nat. Commun.* **10**, 1242 (2019).
25. Walczak, C. P. et al. Ribosomal protein RPL26 is the principal target of UFMylation. *Proc. Natl Acad. Sci. USA* **116**, 1299–1308 (2019).
26. Wang, L. et al. UFMylation of RPL26 links translocation-associated quality control to endoplasmic reticulum protein homeostasis. *Cell Res.* **30**, 5–20 (2020).
27. Nakamura, S., Roth, J. A. & Mukhopadhyay, T. Multiple lysine mutations in the C-terminal domain of p53 interfere with MDM2-dependent protein degradation and ubiquitination. *Mol. Cell Biol.* **20**, 9391–9398 (2000).
28. Rodriguez, M. S., Desterro, J. M., Lain, S., Lane, D. P. & Hay, R. T. Multiple C-terminal lysine residues target p53 for ubiquitin–proteasome-mediated degradation. *Mol. Cell Biol.* **20**, 8458–8467 (2000).
29. Kruse, J. P. & Gu, W. MSL2 promotes Mdm2-independent cytoplasmic localization of p53. *J. Biol. Chem.* **284**, 3250–3263 (2009).
30. Chen, J., Marechal, V. & Levine, A. J. Mapping of the p53 and mdm-2 interaction domains. *Mol. Cell Biol.* **13**, 4107–4114 (1993).
31. Yuan, J., Luo, K., Zhang, L., Cheville, J. C. & Lou, Z. USP10 regulates p53 localization and stability by deubiquitinating p53. *Cell* **140**, 384–396 (2010).
32. Noon, A. P. et al. p53 and MDM2 in renal cell carcinoma: biomarkers for disease progression and future therapeutic targets? *Cancer* **116**, 780–790 (2010).
33. Riley, T., Sontag, E., Chen, P. & Levine, A. Transcriptional control of human p53-regulated genes. *Nat. Rev. Mol. Cell Biol.* **9**, 402–412 (2008).
34. Hu, W., Feng, Z. & Levine, A. J. The regulation of multiple p53 stress responses is mediated through MDM2. *Genes Cancer* **3**, 199–208 (2012).
35. Dai, C. & Gu, W. p53 post-translational modification: deregulated in tumorigenesis. *Trends Mol. Med.* **16**, 528–536 (2010).
36. Beckerman, R. et al. Lysines in the tetramerization domain of p53 selectively modulate G1 arrest. *Cell Cycle* **15**, 1425–1438 (2016).

Methods

Cell culture and reagents. HEK293T and HeLa cells were maintained in Dulbecco's modified Eagle medium (Biological Industries) with 10% foetal bovine serum (FBS; HyClone). U2OS and HCT116 cells were maintained in McCoy's 5A medium (Biological Industries) with 10% FBS. All of these cell lines were purchased from the American Type Culture Collection. The primary MEF cells were isolated and cultured in Dulbecco's modified Eagle medium with 10% FBS, as described[37]. The antibodies used in this study included anti-Flag (Sigma–Aldrich (F7425) and Cell Signaling Technology (2368S)), anti-UFL1 (Sigma–Aldrich; HPA030559), anti-DDRGK1 (Sigma–Aldrich; HPA013373), anti-UFM1 (Abcam; ab109305), anti-p53 (Santa Cruz (sc-126), Abcam (ab26) and Cell Signaling Technology (9282S and 32532S)), anti-p21 (BD Biosciences; 556431), anti-HA (Cell Signaling Technology; 3724S), anti-MDM2 (Cell Signaling Technology; 86934S), anti-Ubiquitin (Millipore; AB1690), anti-γH2AX (Millipore; 05-636), anti-GAPDH (HuaAn Biotechnology; EM1101), normal mouse IgG (Santa Cruz; sc-2025) and normal rabbit IgG (Santa Cruz; sc-2027). The siRNAs targeting *UFL1* and *DDRGK1* were a mixture of two siRNAs purchased from GenePharma. The antibodies used in this study are described in Supplementary Table 4. The sense sequences of siRNAs, as previously reported[38], were as follows: *UFL1*-1: GGAACUUGUUAAUAGCGGA; *UFL1*-2: GAGGAGUAAUUUUUACGGA; *DDRGK1*-1: GAAAAUUGGAGCUAAGAAA; *DDRGK1*-2: CCAUAAAUCGCAUCCAGGA. Etoposide (E1383) was purchased from Sigma–Aldrich; doxorubicin (HY-15142) was purchased from MedChemExpress; and MG132 and cycloheximide were purchased from Beyotime.

Plasmid transfection. UBA5, UFC1, UFL1 and UFM1 complementary DNAs (cDNAs) were cloned into pSG5-HA vector. Mutant UFM1 cDNA with a deletion of two or three amino acids at the C terminus ($UFM1^{\Delta C2}$ or $UFM1^{\Delta C3}$) and with the Lys-less mutation ($UFM1^{K0}$) were cloned into the pSG5-HA vector. DDRGK1 and UFL1 cDNAs were cloned into p3×FLAG-CMV (Sigma–Aldrich) and pcDNA3.1 (Invitrogen) vectors. p53 cDNA was cloned into the pcDNA3.0-3×Flag-6×His vector and the Lys-to-Arg mutations in p53 were generated by site-directed mutagenesis. p53 cDNA and its 4KR mutant were cloned into the pCDH-CMV-EF1 lentivirus expression vector (System Biosciences) for stable cell line generation. Bacteria expressing glutathione *S*-transferases (GST)-tagged UFL1 and DDRGK1 were generated using the pGEX-6P-1 (GE Healthcare) system. All of the constructs were verified via DNA sequencing and are listed in Supplementary Table 5. Plasmid transfection and RNA interference were performed with Lipofectamine 2000 (Invitrogen), according to the manufacturer's instructions.

Assays for UFMylation in vivo and in vitro. For the in vivo UFMylation assay, HEK293T cells were harvested after transfected with the appropriate constructs for 36 h. Cells were lysed by boiling in buffer (150 mM Tris-HCl (pH 8.0), 5% sodium dodecyl sulfate (SDS) and 30% glycerol) for 10 min. Cell lysates were diluted 20-fold with buffer A (50 mM Tris-HCl (pH 8.0), 150 mM NaCl, 0.5% NP-40 and 2 mM *N*-ethylmaleimide) and protease inhibitor cocktails (Roche), as described[13]. After incubation with anti-Flag M2 Affinity Gel (Sigma–Aldrich) overnight at 4 °C, the immunoprecipitates were subjected to SDS polyacrylamide gel electrophores (SDS-PAGE) followed by western blot analysis. For the detection of endogenous p53 UFMylation, U2OS, HCT116 and primary MEF cells were treated with MG132 (20 μg ml^{-1}) for 8 h before harvesting. Cells were lysed by boiling in buffer (150 mM Tris-HCl (pH 8.0), 1% SDS and 30% glycerol) and diluted ten-fold with buffer A followed by precipitation overnight at 4 °C using either a normal mouse IgG (Santa Cruz; sc-2025; 4 or 10 μg) or p53 antibody (Santa Cruz; sc-126; 4 μg) in U2OS and HCT116 cells, or p53 antibody (Abcam; ab26; 10 μg) in primary MEF cells. The immunoprecipitates were then subjected to SDS-PAGE followed by western blot analysis.

In vitro UFMylation assay was performed as described previously[6]. GST-tagged UFL1 and DDRGK1 were ectopically expressed in BL21 cells and purified using Glutathione Sepharose (GE Healthcare). The GST tag was removed using PreScission Protease (Beyotime). Recombinant human His-UBA5 (E-319), His-UFC1 (E2-675), His-UFM1 (UL-500) and p53 protein (SP-454) were obtained from R&D Systems. His-UBA5 (0.1 μM), His-UFC1 (0.1 μM), UFL1 (0.1 μM), DDRGK1 (0.1 μM) and p53 (0.1 μM) were mixed in a reaction buffer (0.05% bovine serum albumin and 50 mM HEPES (pH 7.5)) containing 5 mM ATP and 10 mM $MgCl_2$ and incubated at 30 °C for 2 h. The mixtures were boiled with the addition of SDS sample buffer containing 5% mercaptoethanol for 10 min.

Ubiquitination assay. HCT116 cells were treated with 20 μM MG132 for 8 h before harvesting. Cells were lysed by boiling in buffer (1×phosphate-buffered saline (PBS), 1% NP-40, 0.5% sodium deoxycholate, 1% SDS, 10 mM *N*-ethylmaleimide, 1 mM phenylmethylsulfonyl fluoride, 1 mM NaV_3O_4 and 1 mM NaF) for 10 min. Cell lysates were diluted ten-fold with lysis buffer without SDS and subjected to immunoprecipitation with p53 antibody (Santa Cruz; sc-126). The ubiquitination of endogenous p53 was detected by western blot.

Mass spectrometry. HEK293T cells were transfected with Flag-tagged UFL1, DDRGK1 and p53 for 36 h. The cells were lysed with lysis buffer (50 mM Tris-HCl (pH 7.5), 150 mM NaCl, 1 mM ethylenediaminetetraacetic acid and 0.5% NP-40). Flag-UFL1, Flag-DDRGK1 or Flag-p53 was immunoprecipitated by incubation with anti-FLAG M2 Affinity Gel overnight at 4 °C. Flag-UFL1, Flag-DDRGK1 or Flag-p53 immunoprecipitates were resolved by SDS-PAGE and subjected to mass spectrometry on a Q Exactive HF Mass Spectrometer (Thermo Fisher Scientific). The mass spectrometry analysis was performed by Micrometer Biotech Company, and the candidate proteins for UFMylation are shown in Supplementary Tables 1–3.

GST pulldown and immunoprecipitation. For the in vitro binding assays, purified GST-tagged UFL1 or DDRGK1 was incubated with p53 protein (SP-454; R&D Systems). Reversely, GST-tagged p53 (Abcam; ab43615) was incubated with UFL1 or DDRGK1 proteins prepared using the TNT Translation System (Promega; L1170) in PBS with 0.2% NP-40 for 2 h at 4 °C. A co-immunoprecipitation assay was performed as previously described[21]. Briefly, the harvested cells were lysed in lysis buffer with protease inhibitor cocktail and immunoprecipitated with the appropriate antibodies followed by western blot analysis. The whole-cell lysates as input were included as a control.

For competitive binding assays in vitro, 100 ng UFL1 was incubated with 100 ng immobilized GST-p53 at 4 °C overnight, then incubated with 100, 200 or 400 ng MDM2 for 30 min. The mixtures were boiled with SDS sample buffer and detected by western blot.

Quantitative real-time PCR. Total RNA was extracted from the cells using the TRIzol reagent (Invitrogen) according to the manufacturer's instructions, followed by cDNA preparation using M-MLV reverse transcriptase (Promega). The real-time PCR assays were performed in triplicate using SYBR Green Supermix (Bio-Rad) with the CFX96 Real-Time PCR Detection System (CFX Manager; Bio-Rad). The sequences of the primers employed for real-time PCR are described in Supplementary Table 6.

Stable cell line generation. To harvest lentivirus containing shRNA against UFL1 and DDRGK1, HEK293T cells were transfected with shRNA-expressing plasmids (LV10-U6 vector; GenePharma), together with pLP1, pLP2 and pLP/VSVG. To harvest lentivirus expressing p53 and its mutants, HEK293T cells were transfected with constructs containing cDNA of p53 and its mutants in pCDH-CMV-EF1 vector, together with psPAX2 and pMD2.G. Then, 48 h after transfection, the culture medium was collected to harvest virus particles. HCT116 cells were infected with lentivirus containing shRNAs or cDNAs, and stable cell lines were generated by puromycin (1 μg ml^{-1}) selection.

Colony formation assay. HCT116 cells were seeded into 12-well plates at a density of 2,000 cells per well, and cultured in complete medium for 7 d, followed by treatment with vehicle (dimethyl sulfoxide) or DNA damage inducers (doxorubicin or etoposide) for 2 d. Cells were fixed and then stained by 0.1% crystal violet solution. Stained colonies were imaged and the relative colony intensity was quantitated using the ImageJ image processing program.

Xenograft animal model. Six-week-old BALB/c male nude mice were used in the xenograft experiments. They were randomly allocated into six groups, each of which consisted of nine to 13 nude mice (up to five mice per cage). They were housed under conventional laboratory conditions at a room temperature maintained at 25 ± 1 °C with a relative humidity range of 40–75% and a regular 12 h light/12 h dark cycle. The mice were fed with a standard animal pellet diet and allowed free access to water. HCT116 stable cells were implanted into the dorsal flanking sites of nude mice at 5×10^6 cells in 200 μl PBS. Two weeks after injection, mice bearing tumours were sacrificed by cervical dislocation for the assessment of tumour size and weight examination. All animal experiments were performed according to the guidelines of the Animal Care and Use Committee of Hangzhou Normal University. This study was compliant with all of the relevant ethical regulations regarding animal research.

Tissue microarray and immunohistochemistry. The tissue arrays of kidney cancer samples were purchased from Alenabio (KD 801). Immunohistochemical staining of UFL1 (Abnova; PAB22460; dilution: 1:100), DDRGK1 (Proteintech; 21445-1-AP; dilution: 1:800) and p53 (dilution: 1:100) was carried out with the SP Rabbit & Mouse HRP Kit (CW2069; CWBIO). An Olympus BX63 microscope was used to collect the immunohistochemistry images. The immunostaining was scored by pathologists in a blinded manner. A four-tier grading system of staining intensity (0 = negative; 1 = weak; 2 = moderate; 3 = strong) was used. The normal proximal convoluted tubule showed strong cytoplasmic staining and served as an internal control for strong staining (score 3).

Tissue samples for western blot analysis. Twelve paired tumour tissues and adjacent normal tissues were collected from patients with primary kidney renal clear cell carcinoma at the Department of Pathology, Cancer Hospital of the University of Chinese Academy of Sciences. None of the patients received preoperative treatment. All samples were immediately snap-frozen in liquid nitrogen following surgery and stored in liquid nitrogen for further western blot analysis. The study was approved by the ethics committees of the Cancer Hospital

of the University of Chinese Academy of Sciences, with informed consent from patients. The study was compliant with all of the relevant ethical regulations regarding research involving human participants. Information on the human research participants of this study is provided in Supplementary Table 7.

Statistics and reproducibility. The VersaDoc imaging system (MP 5000; Bio-Rad) was used to collect the western blot images, and ImageJ 1.44p was used for image processing and calculation of colony intensity. GraphPad Prism 5 and 8 and Excel 2007 software was used for all of the statistical analysis. PASW Statistics 18 was used for immunohistochemistry image analysis. A Student's two-tailed *t*-test was used in Fig. 4b,d,f,h,j,l and Extended Data Fig. 4a,b. A two-way analysis of variance test was used for Fig. 3d–i. Person's correlation analysis was used for Fig. 5c. A chi-squared test was used for Extended Data Fig. 6d. For consistency in these comparisons, $P < 0.05$ was considered significant ($^{*}P < 0.05$; $^{**}P < 0.01$; $^{***}P < 0.001$). Each experiment was repeated independently with similar results.

Reporting Summary. Further information on research design is available in the Nature Research Reporting Summary linked to this article.

Data availability

All of the source data supporting the findings of this study are available within this paper and/or from the corresponding author upon reasonable request. The human kidney renal clear cell carcinoma data were derived from The Cancer Genome Atlas Research Network (http://cancergenome.nih.gov/). Source data are provided with this paper.

References

37. Xu, J. Preparation, culture, and immortalization of mouse embryonic fibroblasts. *Curr. Protoc. Mol. Biol.* https://doi.org/10.1002/0471142727.mb2801s70 (2005).

38. Wu, J., Lei, G., Mei, M., Tang, Y. & Li, H. A novel C53/LZAP-interacting protein regulates stability of C53/LZAP and DDRGK domain-containing protein 1 (DDRGK1) and modulates NF-κB signaling. *J. Biol. Chem.* **285**, 15126–15136 (2010).

Acknowledgements

We thank X. Li for providing the MDM2 and ubiquitin constructs, X. Xu for the UFM1 Lys-less construct and S. Bacchetti for critical reading of the manuscript. This work was supported by grants from the National Natural Science Foundation of China (31730020, 31871416, 81701380 and 31571409), Natural Science Foundation of Zhejiang Province of China (LY18C070001 and LY20H250002) and Hangzhou Science and Technology Bureau (20182014B01 and 20180533B27).

Author contributions

J.L., D.G. and Y.-S.C. conceived of and designed the experiments. J.L., D.G., M.D., J.Y., H.W., L.S., L.X., J.B., C.L., Q.L. and J.Z. carried out the experiments. J.L., D.G., J.M., Q.Z., X.W., M.W. and Y.-S.C. analysed and interpreted the data. J.L., D.G. and Y.-S.C. wrote the paper.

Competing interests

The authors declare no competing interests.

Additional information

Extended data is available for this paper at https://doi.org/10.1038/s41556-020-0559-z.

Supplementary information is available for this paper at https://doi.org/10.1038/s41556-020-0559-z.

Correspondence and requests for materials should be addressed to Y.-S.C.

Reprints and permissions information is available at www.nature.com/reprints.

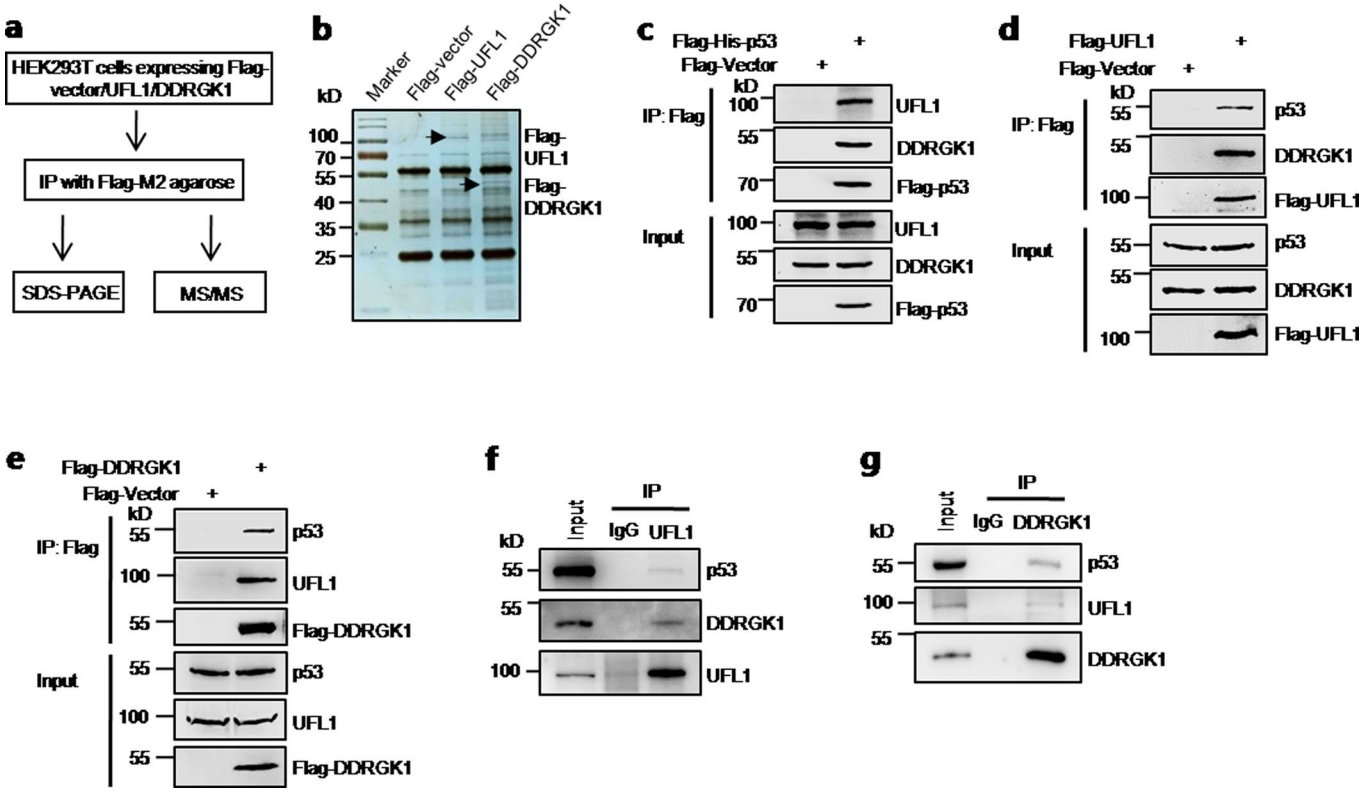

Extended Data Fig. 1 | p53 interacts with UFL1 and DDRGK1. a, Strategy for identification of binding proteins for UFL1 or DDRGK1. **b**, Proteins eluted from anti-Flag M2 affinity gel were subjected to SDS-PAGE followed by silver staining. **c-e**, Western blot analysis of the mutual interactions between p53, UFL1 and DDRGK1 in HEK293T cells by co-immunoprecipitation with anti-Flag M2 affinity gel. **f**, **g**, Western blot analysis of the mutual interactions between UFL1, DDRGK1 and p53 in HEK293T cells by co-immunoprecipitation with UFL1 (**f**) or DDRGK1 (**g**) antibody. Source data are available online.

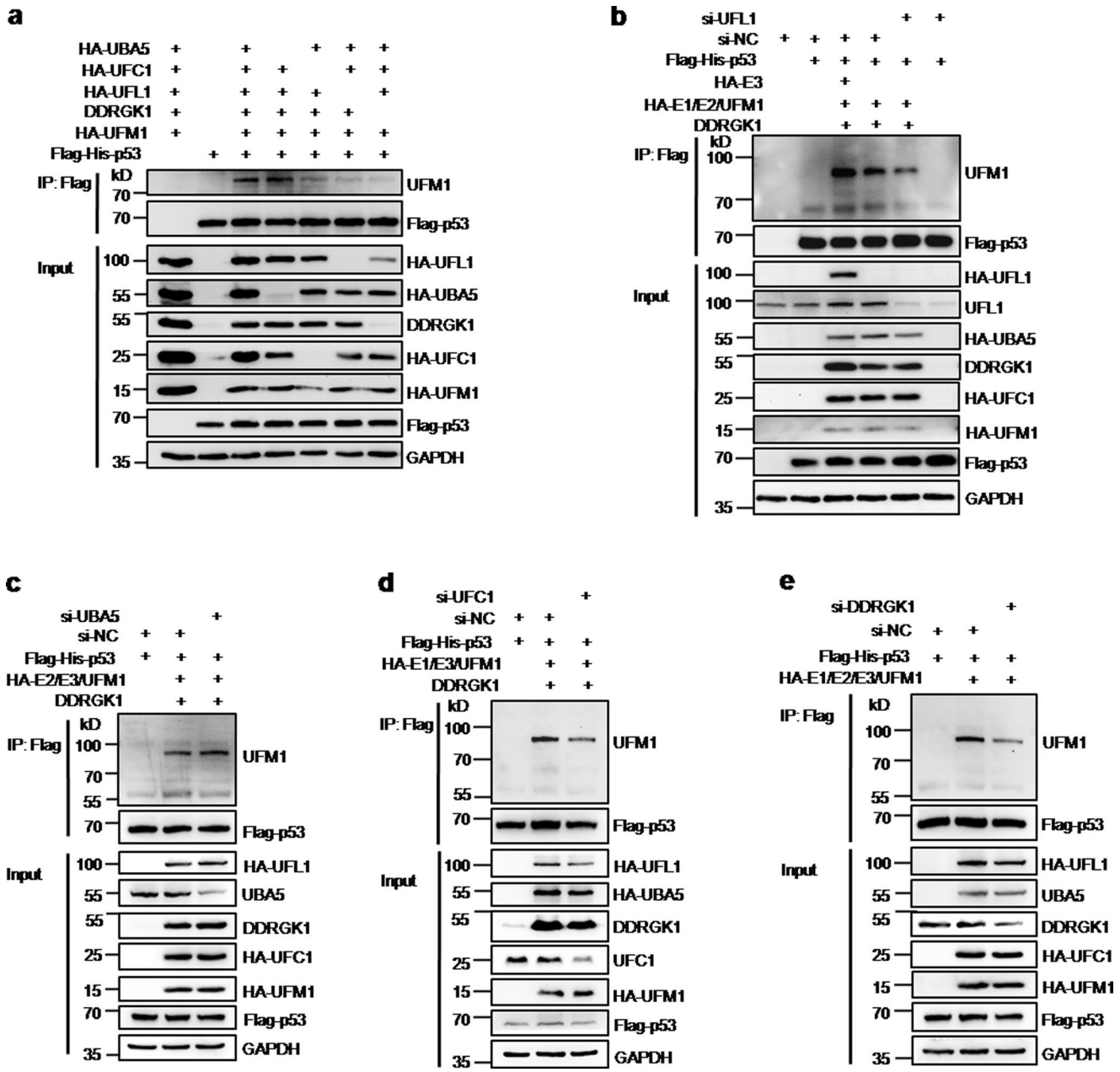

Extended Data Fig. 2 | The effects of UBA5, UFC1, UFL1, and DDRGK1 on p53 ufmylation in cells. a, Western blot analysis of p53 ufmylation in HEK293T cells expressed the ufmylation system components in various combinations as indicated. **b-e**, Western blot analysis of p53 ufmylation in HEK293T cells with depletion of UFL1 (**b**), UBA5 (**c**), UFC1 (**d**), or DDRGK1 (**e**), respectively as indicated. Source data are available online.

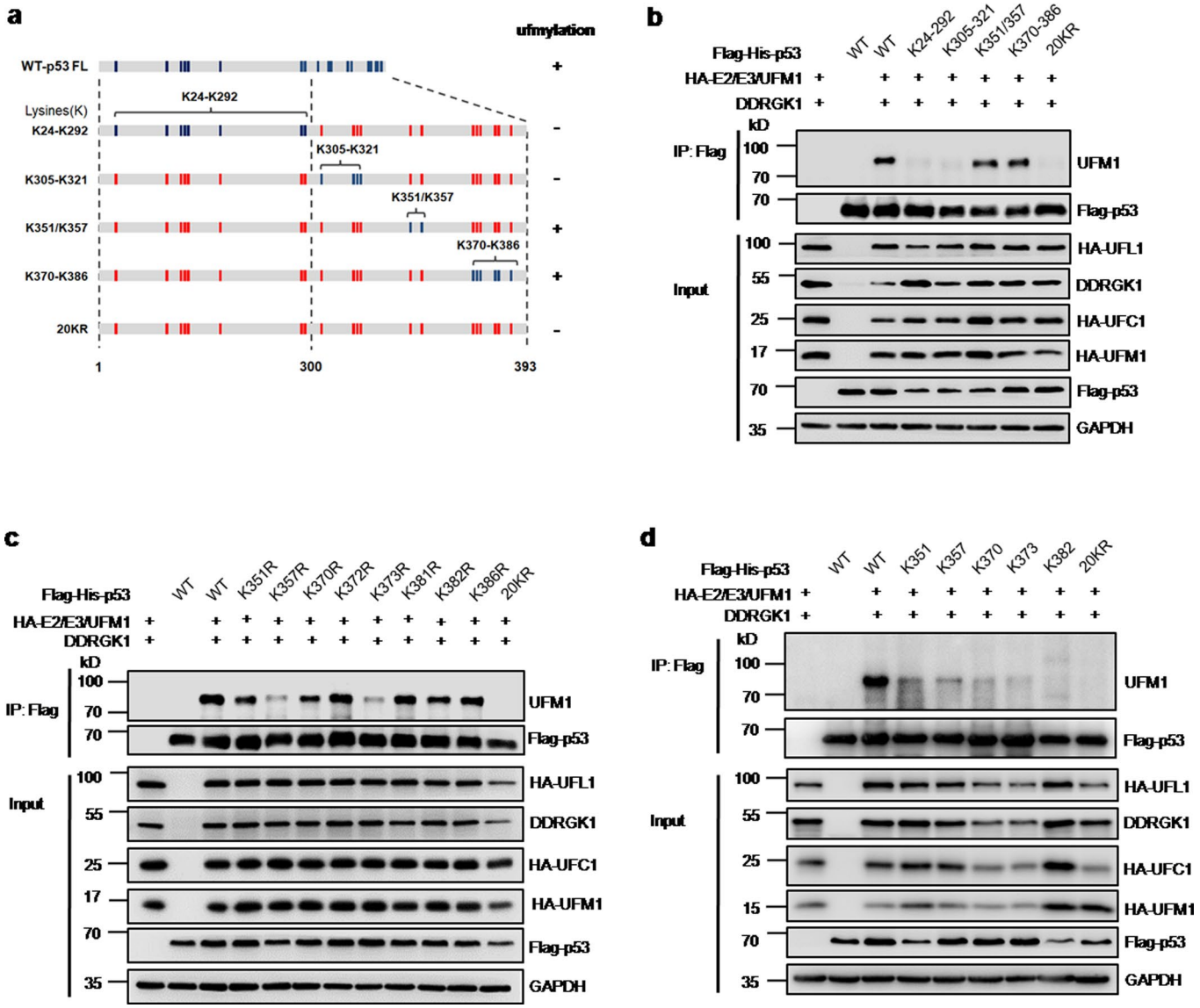

Extended Data Fig. 3 | p53 is ufmylated at Lys351, 357, 370 and 373 of C-terminal region. a, The scheme diagram of p53-WT and its mutants. The Lys residues in p53 were replaced by Arg at the indicated positions. **b**, The ufmylation assay was performed to identity the ufmylation region of p53 in HEK293T cells expressed with p53-WT and its mutants as indicated in (a). **c**, Lys residues were replaced by Arg at indicated positions, and the ufmylation assay was performed in HEK293T cells. **d**, All Lys residues were replaced by Arg in p53 except one each of the five residues Lys351, 357, 370, 373 or 382 as indicated, and the ufmylation assay was performed in HEK293T cells. Source data are available online.

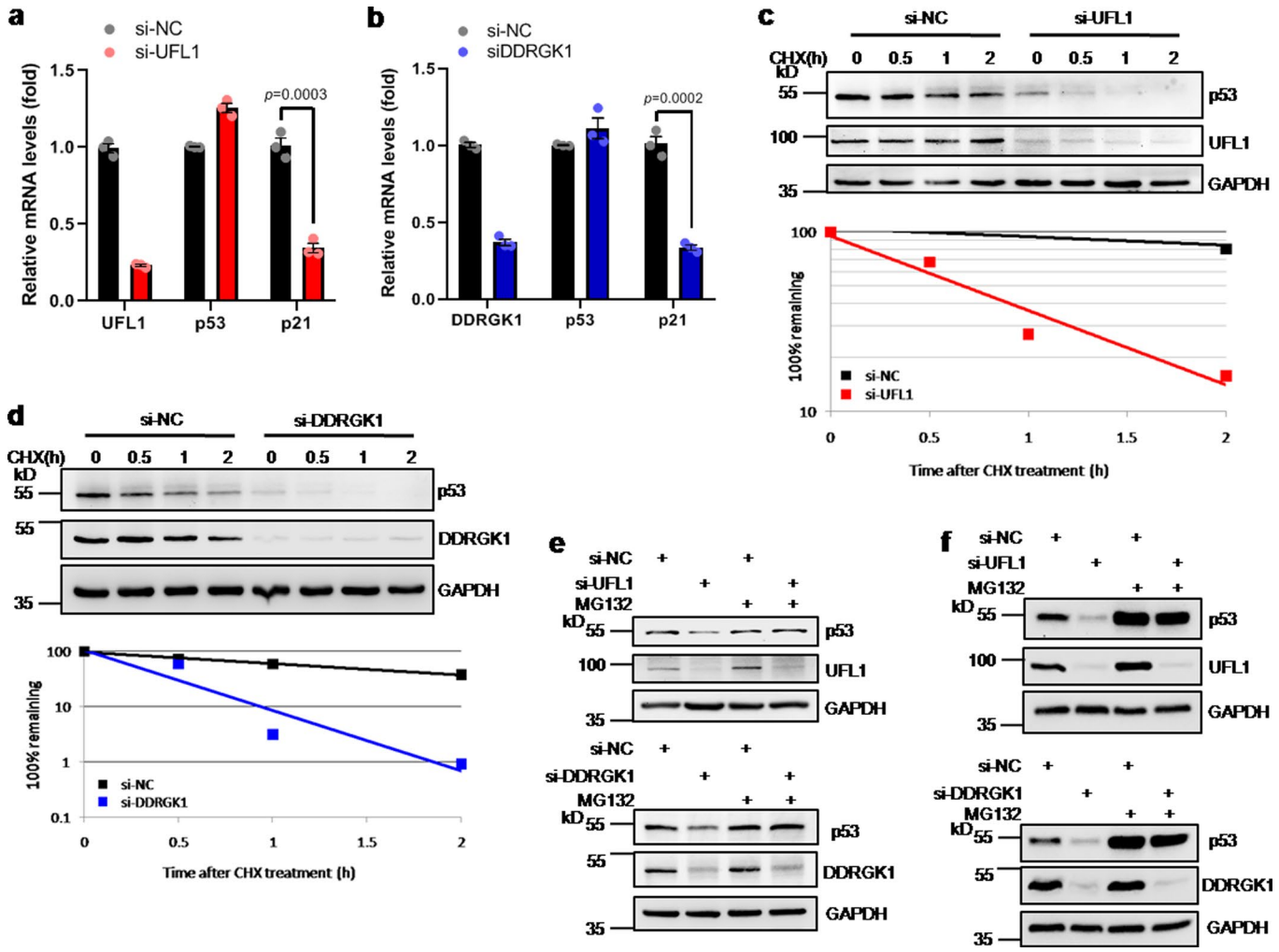

Extended Data Fig. 4 | Ufmylation maintains p53 stability. a, **b**, Q-PCR analysis of the relative mRNA expression of p53 and p21 in HeLa cells with UFL1 depletion (**a**), or DDRGK1 depletion (**b**). Error bars indicate mean ± s.e.m., n=3 for biological replicates. **c**, **d**, p53 stability was examined by western blot in HeLa cells with UFL1 (**c**), or DDRGK1 (**d**) depletion. The cells were treated with 100 μg ml^{-1} CHX for the indicated times, and the graph represents the quantification of the p53 protein levels. **e**, **f**, Western blot analysis of p53 expression in HCT116 (**e**), and HeLa (**f**) cells with UFL1 or DDRGK1 depletion in presence of MG132 (20 μM, 8 h). Source data are available online.

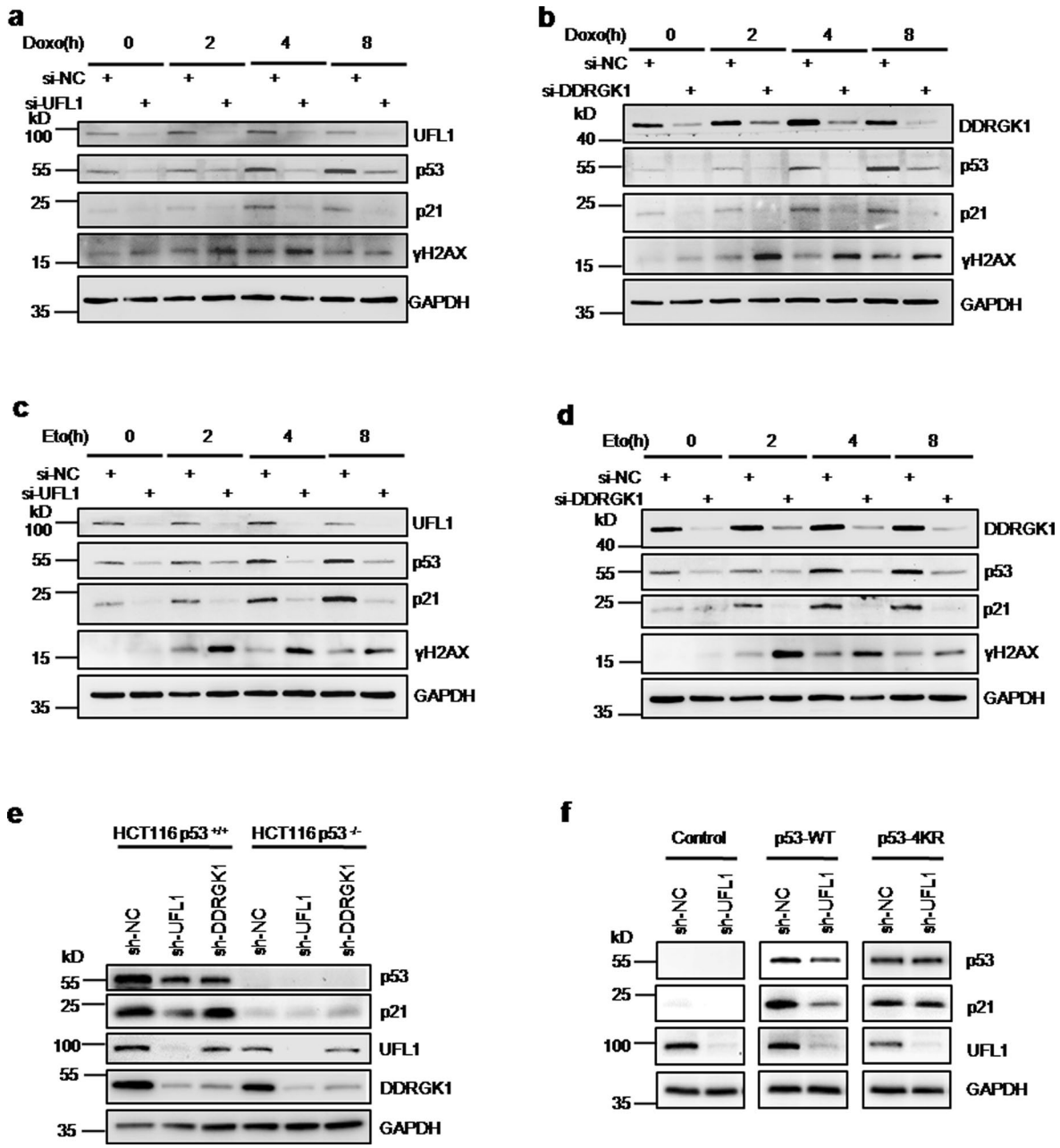

Extended Data Fig. 5 | Ufmylation is required for p53 accumulation in DNA damage response. a–d, Western blot analysis of p53 and p21 expression in HeLa cells with UFL1 or DDRGK1 depletion under DNA damage conditions (Doxo, 1 μM; Eto, 50μM) for indicated time. **e**, Western blot analysis of p53 and p21 expression in HCT116 $p53^{+/+}$ and HCT116 $p53^{-/-}$ cells stably depletion of UFL1 or DDRGK1. **f**, Western blot analysis of p53 and p21 expression in HCT116 $p53^{-/-}$ cells stably expression of p53-WT or p53-4KR with UFL1 depletion. Source data are available online.

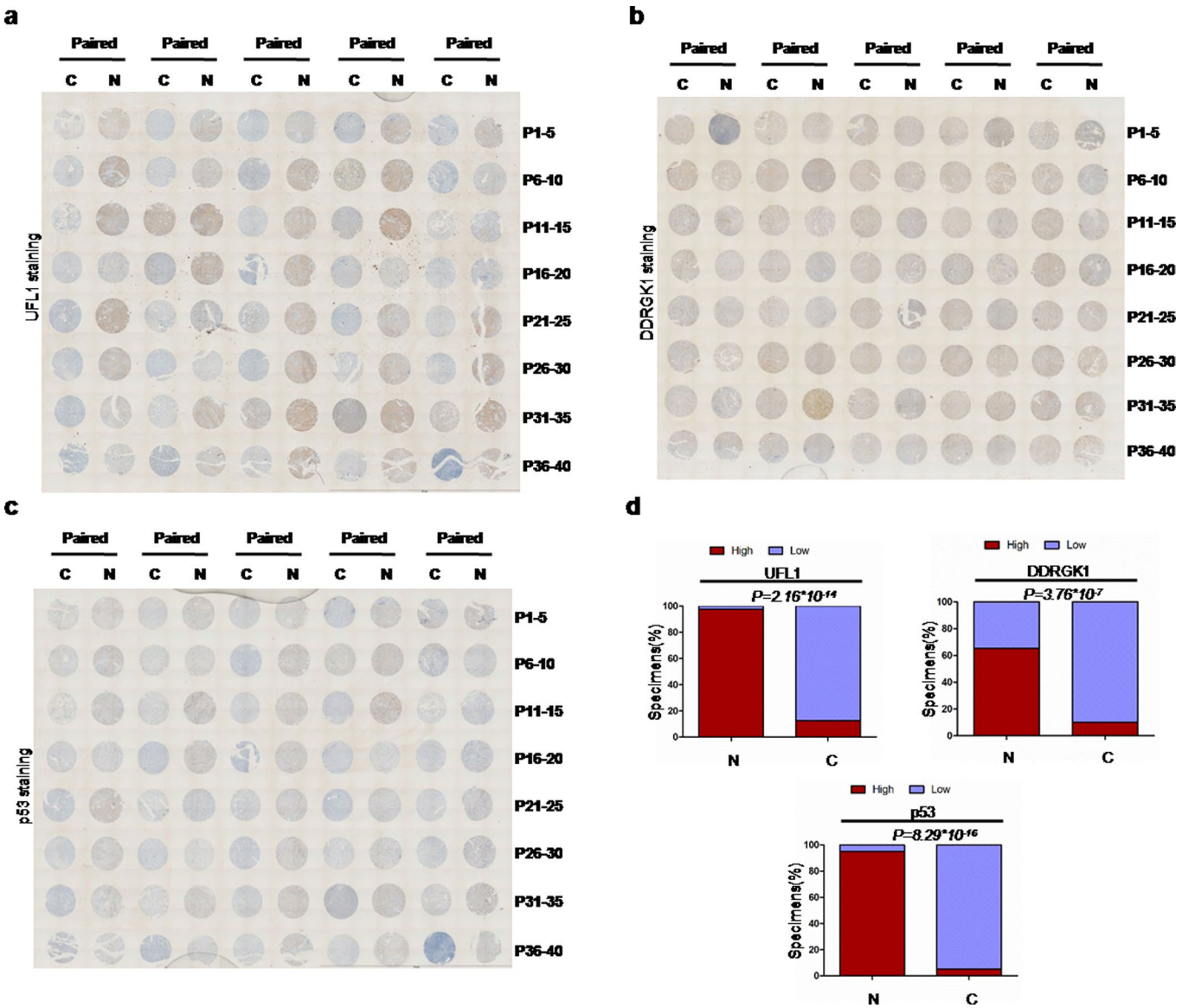

Extended Data Fig. 6 | UFL1 and DDRGK1 are downregulated in renal cell carcinoma. a-c, Immunohistochemical staining of UFL1 (**a**), DDRGK1 (**b**) and p53 (**c**) expression in forty pairs of RCC and adjacent normal tissues in tissue array. **d**, Percentages of the RCC specimens (**a-c**) showed low or high UFL1, DDRGK1 and p53 expression. (N, Normal tissue; C, cancer tissue). *P* values by a Chi-square ($\chi 2$) test, UFL1, $P=2.16*10^{-14}$; DDRGK1, $P=3.76*10^{-7}$; p53, $P=8.29*10^{-16}$. Source data are available online.

nature research

Corresponding author(s): Yu-Sheng Cong

Last updated by author(s): Jun 2, 2020

Reporting Summary

Nature Research wishes to improve the reproducibility of the work that we publish. This form provides structure for consistency and transparency in reporting. For further information on Nature Research policies, see Authors & Referees and the Editorial Policy Checklist.

Statistics

For all statistical analyses, confirm that the following items are present in the figure legend, table legend, main text, or Methods section.

n/a	Confirmed	
☐	☒	The exact sample size (*n*) for each experimental group/condition, given as a discrete number and unit of measurement
☐	☒	A statement on whether measurements were taken from distinct samples or whether the same sample was measured repeatedly
☐	☒	The statistical test(s) used AND whether they are one- or two-sided *Only common tests should be described solely by name; describe more complex techniques in the Methods section.*
☒	☐	A description of all covariates tested
☒	☐	A description of any assumptions or corrections, such as tests of normality and adjustment for multiple comparisons
☐	☒	A full description of the statistical parameters including central tendency (e.g. means) or other basic estimates (e.g. regression coefficient) AND variation (e.g. standard deviation) or associated estimates of uncertainty (e.g. confidence intervals)
☐	☒	For null hypothesis testing, the test statistic (e.g. *F*, *t*, *r*) with confidence intervals, effect sizes, degrees of freedom and *P* value noted *Give P values as exact values whenever suitable.*
☒	☐	For Bayesian analysis, information on the choice of priors and Markov chain Monte Carlo settings
☒	☐	For hierarchical and complex designs, identification of the appropriate level for tests and full reporting of outcomes
☒	☐	Estimates of effect sizes (e.g. Cohen's *d*, Pearson's *r*), indicating how they were calculated

Our web collection on statistics for biologists contains articles on many of the points above.

Software and code

Policy information about availability of computer code

Data collection	Q-PCR data were acquired with CFX96 Real-Time PCR Detection System (CFX Manager, Bio-Rad), Western Blots data were acquired with VersaDoc imaging system (MP 5000, Bio-Rad). IHC images were collected with microscope Olympus BX63 (Olympus).
Data analysis	GraphPad Prism5 and 8 and Excel 2007 were used for all statistical assessments. ImageJ version 1.44P was used for blots quantification and colony intensity calculation. PASW Statistics 18 was used for IHC images analysis.

For manuscripts utilizing custom algorithms or software that are central to the research but not yet described in published literature, software must be made available to editors/reviewers. We strongly encourage code deposition in a community repository (e.g. GitHub). See the Nature Research guidelines for submitting code & software for further information.

Data

Policy information about availability of data

All manuscripts must include a data availability statement. This statement should provide the following information, where applicable:

- Accession codes, unique identifiers, or web links for publicly available datasets
- A list of figures that have associated raw data
- A description of any restrictions on data availability

All source data supporting the findings of this study are available in the paper, and/or from the corresponding author on reasonable request. Statistics source data for statistical analyses in Figures 2b, 3d-i, 4b, d, f, h, j, l, 5c-e, and Extended data figures 4a-d, and 6d are provided in Statistics Source Data. Unprocessed scans of blots and gels are shown in Source Data.

Field-specific reporting

Please select the one below that is the best fit for your research. If you are not sure, read the appropriate sections before making your selection.

☒ Life sciences ☐ Behavioural & social sciences ☐ Ecological, evolutionary & environmental sciences

For a reference copy of the document with all sections, see nature.com/documents/nr-reporting-summary-flat.pdf

Life sciences study design

All studies must disclose on these points even when the disclosure is negative.

Sample size	No statistical method was used to predetermine sample size. The sample sizes were determined according to standards and our experience in the field. For mouse xenograft analysis, a minimum of 9 mice per experimental group. For the work with patients samples, sample sizes were listed in the corresponding figure legend.
Data exclusions	No data were excluded from the analyses.
Replication	Multiple, independent experiments were performed by different researchers to validate the reproducibility of experiments. All attempts at replication were successful.
Randomization	The mice were of the same age, experimental and control cages were randomly assigned.
Blinding	The investigators were not blinded to allocation during experiments and outcome assessment. However, the technician and students who performed the measurement of tumor size and weight were blind to the allocation. Human tissue microarray were scored in a blinded manner prior to analysis by investigators.

Behavioural & social sciences study design

All studies must disclose on these points even when the disclosure is negative.

Study description	*Briefly describe the study type including whether data are quantitative, qualitative, or mixed-methods (e.g. qualitative cross-sectional, quantitative experimental, mixed-methods case study).*
Research sample	*State the research sample (e.g. Harvard university undergraduates, villagers in rural India) and provide relevant demographic information (e.g. age, sex) and indicate whether the sample is representative. Provide a rationale for the study sample chosen. For studies involving existing datasets, please describe the dataset and source.*
Sampling strategy	*Describe the sampling procedure (e.g. random, snowball, stratified, convenience). Describe the statistical methods that were used to predetermine sample size OR if no sample-size calculation was performed, describe how sample sizes were chosen and provide a rationale for why these sample sizes are sufficient. For qualitative data, please indicate whether data saturation was considered, and what criteria were used to decide that no further sampling was needed.*
Data collection	*Provide details about the data collection procedure, including the instruments or devices used to record the data (e.g. pen and paper, computer, eye tracker, video or audio equipment) whether anyone was present besides the participant(s) and the researcher, and whether the researcher was blind to experimental condition and/or the study hypothesis during data collection.*
Timing	*Indicate the start and stop dates of data collection. If there is a gap between collection periods, state the dates for each sample cohort.*
Data exclusions	*If no data were excluded from the analyses, state so OR if data were excluded, provide the exact number of exclusions and the rationale behind them, indicating whether exclusion criteria were pre-established.*
Non-participation	*State how many participants dropped out/declined participation and the reason(s) given OR provide response rate OR state that no participants dropped out/declined participation.*
Randomization	*If participants were not allocated into experimental groups, state so OR describe how participants were allocated to groups, and if allocation was not random, describe how covariates were controlled.*

Ecological, evolutionary & environmental sciences study design

All studies must disclose on these points even when the disclosure is negative.

Study description	*Briefly describe the study. For quantitative data include treatment factors and interactions, design structure (e.g. factorial, nested, hierarchical), nature and number of experimental units and replicates.*
Research sample	*Describe the research sample (e.g. a group of tagged Passer domesticus, all Stenocereus thurberi within Organ Pipe Cactus National*

Research sample	*Monument), and provide a rationale for the sample choice. When relevant, describe the organism taxa, source, sex, age range and any manipulations. State what population the sample is meant to represent when applicable. For studies involving existing datasets, describe the data and its source.*
Sampling strategy	*Note the sampling procedure. Describe the statistical methods that were used to predetermine sample size OR if no sample-size calculation was performed, describe how sample sizes were chosen and provide a rationale for why these sample sizes are sufficient.*
Data collection	*Describe the data collection procedure, including who recorded the data and how.*
Timing and spatial scale	*Indicate the start and stop dates of data collection, noting the frequency and periodicity of sampling and providing a rationale for these choices. If there is a gap between collection periods, state the dates for each sample cohort. Specify the spatial scale from which the data are taken*
Data exclusions	*If no data were excluded from the analyses, state so OR if data were excluded, describe the exclusions and the rationale behind them, indicating whether exclusion criteria were pre-established.*
Reproducibility	*Describe the measures taken to verify the reproducibility of experimental findings. For each experiment, note whether any attempts to repeat the experiment failed OR state that all attempts to repeat the experiment were successful.*
Randomization	*Describe how samples/organisms/participants were allocated into groups. If allocation was not random, describe how covariates were controlled. If this is not relevant to your study, explain why.*
Blinding	*Describe the extent of blinding used during data acquisition and analysis. If blinding was not possible, describe why OR explain why blinding was not relevant to your study.*

Did the study involve field work? ☐ Yes ☐ No

Field work, collection and transport

Field conditions	*Describe the study conditions for field work, providing relevant parameters (e.g. temperature, rainfall).*
Location	*State the location of the sampling or experiment, providing relevant parameters (e.g. latitude and longitude, elevation, water depth).*
Access and import/export	*Describe the efforts you have made to access habitats and to collect and import/export your samples in a responsible manner and in compliance with local, national and international laws, noting any permits that were obtained (give the name of the issuing authority, the date of issue, and any identifying information).*
Disturbance	*Describe any disturbance caused by the study and how it was minimized.*

Reporting for specific materials, systems and methods

We require information from authors about some types of materials, experimental systems and methods used in many studies. Here, indicate whether each material, system or method listed is relevant to your study. If you are not sure if a list item applies to your research, read the appropriate section before selecting a response.

Materials & experimental systems

n/a	Involved in the study
☐	☒ Antibodies
☐	☒ Eukaryotic cell lines
☒	☐ Palaeontology
☐	☒ Animals and other organisms
☐	☒ Human research participants
☒	☐ Clinical data

Methods

n/a	Involved in the study
☒	☐ ChIP-seq
☒	☐ Flow cytometry
☒	☐ MRI-based neuroimaging

Antibodies

Antibodies used	Rabbit polyclonal anti-Flag (Sigma, F7425, lot: 078M4886V, 1:1000) Rabbit polyclonal anti-Flag (Cell Signaling Technology, 2368S, lot: 4, 1:1000) Rabbit polyclonal anti-UFL1 (Sigma, HPA030559, lot: A115342, 1:1000; 4ug) Rabbit polyclonal anti-UFL1 (Abnova, PAB22460, lot: 231068, 1:100) Rabbit polyclonal anti-DDRGK1 (Sigma, HPA013373, lot: A78521, 1:1000; 4ug) Rabbit polyclonal anti-DDRGK1 (Proteintech, 21445-1-AP, 1:800) Rabbit monoclonal anti-UFM1 (EPR4264 (2)) (Abcam, ab109305, lot: GR3206277, 1:1000) Mouse monoclonal anti-p53 (DO-1) (Santa Cruz, sc-126, lot: I2118, 1:1000; 4ug) Rabbit polyclonal anti-p53 (Cell Signaling Technology, 9282S, lot: 4, 1: 1000) Rabbit monoclonal anti-p53 (D2H9O) (Cell Signaling Technology, 32532S, lot: 2, 1: 1000) Mouse monoclonal anti-p53 (PAB240) (Abcam, ab26, lot: GR3213177-1; 10ug)

Mouse monoclonal anti-p21 (SXM30) (BD Biosciences, 556431, lot: 7271524, 1:1000)
Rabbit monoclonal anti-HA (C29F4) (Cell Signaling Technology, 3724S, lot: 2, 1: 1000)
Rabbit monoclonal anti-MDM2 (D1V2Z) (Cell Signaling Technology, 86934S, lot: 2, 1: 1000)
Rabbit polyclonal anti-Ubiquitin (Millipore, AB1690, lot: 3032765, 1: 1000)
Mouse monoclonal anti-γH2AX (JBW301) (Millipore, 05-636, lot: DAM1405597, 1: 1000)
Mouse monoclonal anti-GAPDH (5-E10) (HuaAn Biotechnology, HG0718, lot: EM1101, 1: 5000).
Normal mouse IgG (Santa Cruz, sc-2025, lot: K1017, 4ug, 10ug)
Normal Rabbit IgG (Santa Cruz, sc-2027, lot: L2414, 4ug)
Antibody information is provided in Supplementary Table 2.

Validation

Rabbit polyclonal anti-Flag (Sigma): western blot (WB), see manufacturer's website for references
Rabbit polyclonal anti-Flag (Cell Signaling Technology): WB, see manufacturer's website for references
Rabbit polyclonal anti-UFL1 (Sigma): WB, immunoprecipitation (IP), see manufacturer's website for references
Rabbit polyclonal anti-UFL1 (Abnova): immunohistochemistry (IHC), see manufacturer's website for references
Rabbit polyclonal anti-DDRGK1 (Sigma): WB, IP, see manufacturer's website for references
Rabbit polyclonal anti-DDRGK1 (Proteintech): IHC, see manufacturer's website for references
Rabbit monoclonal anti-UFM1: WB, see manufacturer's website for references
Mouse monoclonal anti-p53 (DO-1): WB, IP, IHC, see manufacturer's website for references
Rabbit polyclonal anti-p53: WB, see manufacturer's website for references
Mouse monoclonal anti-p53 (PAB240): IP, see manufacturer's website for references
Mouse monoclonal anti-p21: WB, see manufacturer's website for references
Rabbit monoclonal anti-HA: WB, see manufacturer's website for references
Rabbit monoclonal anti-MDM2: WB, see manufacturer's website for references
Rabbit polyclonal anti-Ubiquitin: WB, see manufacturer's website for references
Mouse monoclonal anti-γH2AX: WB, see manufacturer's website for references
Mouse monoclonal anti-GAPDH: WB, see manufacturer's website for references
Normal mouse IgG: IP, see manufacturer's website for references
Normal Rabbit IgG: IP see manufacturer's website for references
We further validated anti-Flag, anti-UFL1, anti-DDRGK1, anti-UFM1, anti-p53, anti-p21, anti-MDM2, anti-HA, anti-Ubiquitin, and anti-γH2AX antibodies using knockdown, ectopic expression, or different stimulations by western blotting.

Eukaryotic cell lines

Policy information about cell lines

Cell line source(s)	HEK293T, HeLa, U2OS and HCT116 cell lines were purchased from ATCC, and primary MEF cells were isolated and cultured in the lab.
Authentication	HeLa cell lines were found 100% matched with HeLa cell lines in the ATCC and DSMZ databases by STR DNA profiling analysis, no cross contamination of other human cells was found. The other three cell lines were not authenticated.
Mycoplasma contamination	All cell lines were tested negative for mycoplasma contamination.
Commonly misidentified lines (See ICLAC register)	No commonly misidentified cell lines were used in the study.

Palaeontology

Specimen provenance	*Provide provenance information for specimens and describe permits that were obtained for the work (including the name of the issuing authority, the date of issue, and any identifying information).*
Specimen deposition	*Indicate where the specimens have been deposited to permit free access by other researchers.*
Dating methods	*If new dates are provided, describe how they were obtained (e.g. collection, storage, sample pretreatment and measurement), where they were obtained (i.e. lab name), the calibration program and the protocol for quality assurance OR state that no new dates are provided.*

☐ Tick this box to confirm that the raw and calibrated dates are available in the paper or in Supplementary Information.

Animals and other organisms

Policy information about studies involving animals; ARRIVE guidelines recommended for reporting animal research

Laboratory animals	The 6-week-old BALB/c male nude mice were used in the study.
Wild animals	The study did not involve wild animals.
Field-collected samples	The study did not involve samples collected from field.
Ethics oversight	All animal experiments were performed according to guidelines of Animal Care and Use Committee of Hangzhou Normal University.

Note that full information on the approval of the study protocol must also be provided in the manuscript.

Human research participants

Policy information about studies involving human research participants

Population characteristics	Tumor tissues and the adjacent normal tissues collected from patients with primary kidney renal clear cell carcinoma were used in the study.
Recruitment	The patient samples with primary kidney renal clear cell carcinoma at the Department of Pathology, Cancer Hospital of the University of Chinese Academy of Sciences were used for western blots in the study. No bias expected to affect this study as no outcome data is reported.
Ethics oversight	The study was approved by the Ethics Committees of Cancer Hospital of the University of Chinese Academy of Sciences with informed consent from patients.

Note that full information on the approval of the study protocol must also be provided in the manuscript.

Clinical data

Policy information about clinical studies

All manuscripts should comply with the ICMJE guidelines for publication of clinical research and a completed CONSORT checklist must be included with all submissions.

Clinical trial registration	*Provide the trial registration number from ClinicalTrials.gov or an equivalent agency.*
Study protocol	*Note where the full trial protocol can be accessed OR if not available, explain why.*
Data collection	*Describe the settings and locales of data collection, noting the time periods of recruitment and data collection.*
Outcomes	*Describe how you pre-defined primary and secondary outcome measures and how you assessed these measures.*

ChIP-seq

Data deposition

☐ Confirm that both raw and final processed data have been deposited in a public database such as GEO.

☐ Confirm that you have deposited or provided access to graph files (e.g. BED files) for the called peaks.

Data access links *May remain private before publication.*	*For "Initial submission" or "Revised version" documents, provide reviewer access links. For your "Final submission" document, provide a link to the deposited data.*
Files in database submission	*Provide a list of all files available in the database submission.*
Genome browser session (e.g. UCSC)	*Provide a link to an anonymized genome browser session for "Initial submission" and "Revised version" documents only, to enable peer review. Write "no longer applicable" for "Final submission" documents.*

Methodology

Replicates	*Describe the experimental replicates, specifying number, type and replicate agreement.*
Sequencing depth	*Describe the sequencing depth for each experiment, providing the total number of reads, uniquely mapped reads, length of reads and whether they were paired- or single-end.*
Antibodies	*Describe the antibodies used for the ChIP-seq experiments; as applicable, provide supplier name, catalog number, clone name, and lot number.*
Peak calling parameters	*Specify the command line program and parameters used for read mapping and peak calling, including the ChIP, control and index files used.*
Data quality	*Describe the methods used to ensure data quality in full detail, including how many peaks are at FDR 5% and above 5-fold enrichment.*
Software	*Describe the software used to collect and analyze the ChIP-seq data. For custom code that has been deposited into a community repository, provide accession details.*

Flow Cytometry

Plots

Confirm that:

☐ The axis labels state the marker and fluorochrome used (e.g. CD4-FITC).

☐ The axis scales are clearly visible. Include numbers along axes only for bottom left plot of group (a 'group' is an analysis of identical markers).

☐ All plots are contour plots with outliers or pseudocolor plots.

☐ A numerical value for number of cells or percentage (with statistics) is provided.

Methodology

Sample preparation	*Describe the sample preparation, detailing the biological source of the cells and any tissue processing steps used.*
Instrument	*Identify the instrument used for data collection, specifying make and model number.*
Software	*Describe the software used to collect and analyze the flow cytometry data. For custom code that has been deposited into a community repository, provide accession details.*
Cell population abundance	*Describe the abundance of the relevant cell populations within post-sort fractions, providing details on the purity of the samples and how it was determined.*
Gating strategy	*Describe the gating strategy used for all relevant experiments, specifying the preliminary FSC/SSC gates of the starting cell population, indicating where boundaries between "positive" and "negative" staining cell populations are defined.*

☐ Tick this box to confirm that a figure exemplifying the gating strategy is provided in the Supplementary Information.

Magnetic resonance imaging

Experimental design

Design type	*Indicate task or resting state; event-related or block design.*
Design specifications	*Specify the number of blocks, trials or experimental units per session and/or subject, and specify the length of each trial or block (if trials are blocked) and interval between trials.*
Behavioral performance measures	*State number and/or type of variables recorded (e.g. correct button press, response time) and what statistics were used to establish that the subjects were performing the task as expected (e.g. mean, range, and/or standard deviation across subjects).*

Acquisition

Imaging type(s)	*Specify: functional, structural, diffusion, perfusion.*
Field strength	*Specify in Tesla*
Sequence & imaging parameters	*Specify the pulse sequence type (gradient echo, spin echo, etc.), imaging type (EPI, spiral, etc.), field of view, matrix size, slice thickness, orientation and TE/TR/flip angle.*
Area of acquisition	*State whether a whole brain scan was used OR define the area of acquisition, describing how the region was determined.*

Diffusion MRI ☐ Used ☐ Not used

Preprocessing

Preprocessing software	*Provide detail on software version and revision number and on specific parameters (model/functions, brain extraction, segmentation, smoothing kernel size, etc.).*
Normalization	*If data were normalized/standardized, describe the approach(es): specify linear or non-linear and define image types used for transformation OR indicate that data were not normalized and explain rationale for lack of normalization.*
Normalization template	*Describe the template used for normalization/transformation, specifying subject space or group standardized space (e.g. original Talairach, MNI305, ICBM152) OR indicate that the data were not normalized.*
Noise and artifact removal	*Describe your procedure(s) for artifact and structured noise removal, specifying motion parameters, tissue signals and physiological signals (heart rate, respiration).*
Volume censoring	*Define your software and/or method and criteria for volume censoring, and state the extent of such censoring.*

Statistical modeling & inference

Model type and settings	*Specify type (mass univariate, multivariate, RSA, predictive, etc.) and describe essential details of the model at the first and second levels (e.g. fixed, random or mixed effects; drift or auto-correlation).*
Effect(s) tested	*Define precise effect in terms of the task or stimulus conditions instead of psychological concepts and indicate whether ANOVA or factorial designs were used.*

Specify type of analysis: ☐ Whole brain ☐ ROI-based ☐ Both

Statistic type for inference (See Eklund et al. 2016)	*Specify voxel-wise or cluster-wise and report all relevant parameters for cluster-wise methods.*
Correction	*Describe the type of correction and how it is obtained for multiple comparisons (e.g. FWE, FDR, permutation or Monte Carlo).*

Models & analysis

n/a	Involved in the study
☐	☐ Functional and/or effective connectivity
☐	☐ Graph analysis
☐	☐ Multivariate modeling or predictive analysis

Functional and/or effective connectivity	*Report the measures of dependence used and the model details (e.g. Pearson correlation, partial correlation, mutual information).*
Graph analysis	*Report the dependent variable and connectivity measure, specifying weighted graph or binarized graph, subject- or group-level, and the global and/or node summaries used (e.g. clustering coefficient, efficiency, etc.).*
Multivariate modeling and predictive analysis	*Specify independent variables, features extraction and dimension reduction, model, training and evaluation metrics.*